Efficient time integration for discontinuous Galerkin approximations of linear wave equations

Marlis Hochbruck*, **Tomislav Pažur, Andreas Schulz, Ekkachai Thawinan, and Christian Wieners**

Institute for Applied and Numerical Mathematics, Karlsruhe Institute of Technology

Received XXXX, revised XXXX, accepted XXXX
Published online XXXX

Key words Wave equation, discontinuous Galerkin method, upwind flux, implicit Runge–Kutta methods, exponential integrators, Krylov subspace methods, matrix exponential function.

MSC (2000) 65M20, 65F60, 65M60, 65M12

We consider the combination of discontinuous Galerkin discretizations in space with various time integration methods for linear acoustic, elastic, and electro-magnetic wave equations. For the discontinuous Galerkin method we derive explicit formulas for the full upwind flux for heterogeneous materials by solving the Riemann problems for the corresponding first-order systems. In a framework of bounded semigroups we prove convergence of the spatial discretization.

For the time integration we discuss advantages and disadvantages of explicit and implicit Runge–Kutta methods compared to polynomial and rational Krylov subspace methods for the approximation of the matrix exponential function. Finally, the efficiency of the different time integrators is illustrated by several examples in 2D and 3D for electro-magnetic and elastic waves.

1 Introduction

In the last decade discontinuous Galerkin methods became very popular for first-order hyperbolic systems, cf. [6, 18, 19]. They are now well established in combination with standard explicit Runge-Kutta methods, see, e.g., [4], for an error analysis of the full discretization in the more general case of symmetric Friedrich systems.

In this paper we consider the solution of homogeneous linear acoustic, elastic, and electro-magnetic wave equations by discontinuous Galerkin discretizations in space. For such linear problems, the solution is given as a matrix exponential function multiplied by the vector containing the initial value. We discuss the relation between standard explicit or implicit Runge-Kutta methods and polynomial or rational Krylov subspace methods for approximating the matrix exponential function directly [11, 14, 16, 21, 32]. It is well known that polynomial Krylov subspace methods for the matrix exponential $\exp(\tau A)v$ always converge superlinearly but unfortunately, for the wave equation, the onset of superlinear convergence behavior only starts after $\|\tau A\|$ steps [21]. Nevertheless, these methods have been successfully applied to wave problems, see, e.g., [3,7,30,41]. In contrast, it has been shown recently in [12,14,16] that rational Krylov subspace methods converge independently of $\|\tau A\|$ and even for unbounded operators A. Using implicit methods or rational Krylov approximations is the only possible option to overcome the CFL barrier of explicit schemes or the limitation by the number of steps to reach the superlinear convergence behavior for polynomial Krylov methods. Note that these limitations arise in the same way for uniformly refined grid and for locally refined grid, although for the latter, local time stepping methods are a very attractive alternative, see, e.g., [15, 26, 36]. SPP-RK methods, which became very popular in combination with DG methods suffer from a slightly less stringent CFL restriction, see, e.g., [5, 7, 13, 33].

Our goal is to present a general framework for the construction of discontinuous Galerkin discretizations in space for wave equations and to advocate the combination with modern time integration. Finally, we show for representative examples in this application class that Krylov subspace methods can be significantly more efficient than standard Runge–Kutta schemes, even with a standard implementation which was not optimized for the particular application.

The paper is organized as follows. In Section 2 we discuss acoustic, elastic, and electromagnetic wave equations in a semigroup framework. These problems can be considered as linear systems of conservation laws. In Section 3 we focus on the explicit construction of the exact solution of the Riemann problems (defining the full upwind flux [27]) in case of variable coefficients. In Section 4 we construct the discretized operator for linear systems of conservation laws and the three types of wave equations. We show that the semi-discrete finite volume estimates given in [38] can be transferred

* Corresponding author, e-mail: marlis.hochbruck@kit.edu

to this setting resulting in convergence estimates in space for sufficiently smooth solutions. Estimates for a central flux discontinuous Galerkin discretization of the Maxwell problem are presented in [10].

Different options for the time integration of linear first-order systems are considered in Section 5. We discuss the relations between explicit Runge-Kutta methods and polynomials Krylov subspace methods and between implicit Runge-Kutta methods and rational Krylov subspace methods for the approximation of the matrix exponential. Since Krylov subspace methods have to be implemented with care, we present the full algorithms for the discrete problems resulting from the space discretization by discontinuous Galerkin methods.

In Section 6 we compare the efficiency of the different time integration schemes. For the implicit methods and the rational Krylov method, a parallel multigrid preconditioner [39] is implemented for solving the linear systems.

2 Linear hyperbolic operators for wave equations

In this section we introduce our notation and summarize basic results on wave equations in the framework of semigroup theory, see, e.g., [9]. More precisely, we check the assumptions of the Lumer-Phillips theorem [31, Chap. 12.2.2] for acoustic, elastic, and electro-magnetic waves. This shows that these problems are well-posed and that the initial value problem has a unique solution in a suitable Hilbert space setting.

2.1 The general setting

Let $\Omega \subset \mathbb{R}^D$ be a bounded Lipschitz domain, and let $V \subset \mathrm{L}_2(\Omega, \mathbb{R}^J)$ be a Hilbert space with weighted inner product $(\mathbf{v}, \mathbf{w})_V = (M\mathbf{v}, \mathbf{w})_{0,\Omega}$, where $M \in \mathrm{L}_\infty(\Omega, \mathbb{R}^{J\times J})$ is uniformly positive and symmetric.

We study the evolution equation

$$M\partial_t \mathbf{u}(t) + A\mathbf{u}(t) \quad = \quad 0\,, \qquad t \in [0,T]\,, \qquad \mathbf{u}(0) = \mathbf{u}_0\,. \tag{1}$$

Here, A is a linear operator on V with dense domain $\mathcal{D}(A) \subset V$ corresponding to a hyperbolic linear system, i.e.,

$$(A\mathbf{v}, \mathbf{v})_{0,\Omega} = 0\,, \qquad \mathbf{v} \in \mathcal{D}(A)\,. \tag{2}$$

For simplicity, we consider only homogeneous boundary conditions on $\partial\Omega$ which are included in the domain of the operator.

For our applications, we will show that for any $\mathbf{b} \in V$ a unique solution $\mathbf{v} \in \mathcal{D}(A)$ of $A\mathbf{v} + M\mathbf{v} = M\mathbf{b}$ exists. Then, by the Lumer-Phillips theorem, the operator $M^{-1}A$ generates a continuous semigroup in V, and for any $\mathbf{u}_0 \in \mathcal{D}(A)$ a unique solution of the evolution equation (1) exists. Moreover, the energy $\mathcal{E}(\mathbf{v}) = \frac{1}{2}(\mathbf{v}, \mathbf{v})_V$ satisfies

$$\partial_t \mathcal{E}(\mathbf{u}(t)) = \big(M\partial_t \mathbf{u}(t), \mathbf{u}(t)\big)_{0,\Omega} = -\big(A\mathbf{u}(t), \mathbf{u}(t)\big)_{0,\Omega} = 0,$$

i.e., the energy is conserved $\mathcal{E}(\mathbf{u}(t)) = \mathcal{E}(\mathbf{u}(0))$ for all $t \in [0,T]$.

We study three different applications fitting into this framework, namely acoustic, elastic, and electromagnetic waves.

2.2 Applications

In all applications, the operator A corresponds to a linear system of J first-order differential equations.

Acoustic waves Acoustic waves in an isotropic medium with variable density $\rho \in \mathrm{L}_\infty(\Omega)$ are described by the second-order scalar equation for the potential

$$\rho\partial_t^2 \psi - \Delta\psi = 0\,.$$

We assume $\rho(\mathbf{x}) \geq \rho_0 > 0$ for a.a. $\mathbf{x} \in \Omega$. Introducing the pressure $p = \partial_t\psi$ and the flux $\mathbf{q} = -\nabla\psi$ this corresponds to the first-order system

$$\rho\partial_t p + \operatorname{div}\mathbf{q} = 0\,, \qquad \partial_t \mathbf{q} + \nabla p = \mathbf{0}$$

with $J = D + 1$ components. We define the operators

$$M(\mathbf{q}, p) = (\mathbf{q}, \rho p), \qquad A(\mathbf{q}, p) = (\nabla p, \operatorname{div}\mathbf{q})$$

on the Hilbert space $V = \mathrm{L}_2(\Omega, \mathbb{R}^J)$. In the case of homogeneous Dirichlet boundary conditions, the domain is given by $\mathcal{D}(A) = \mathrm{H}(\operatorname{div}, \Omega) \times \mathrm{H}_0^1(\Omega)$ and thus $\mathcal{D}(A)$ is dense in V.

For the application of the semigroup setting it remains to consider the mapping property of $A + M$. For arbitrarily chosen $(\mathbf{f}, g) \in V$ we consider the stationary problem

$$(M + A)(\mathbf{q}, p) = M(\mathbf{f}, g), \tag{3}$$

which is equivalent to

$$\mathbf{q} + \nabla p = \mathbf{f}\,, \qquad \rho p + \operatorname{div} \mathbf{q} = \rho g. \tag{4}$$

To obtain a variational formulation, we take the divergence of the first equation and insert $\operatorname{div} \mathbf{q}$ into the second. Next, multiplying with a test function $\psi \in H_0^1(\Omega)$ and integrating, yields the elliptic problem for p

$$(\nabla p, \nabla \psi)_{0,\Omega} + (\rho p, \psi)_{0,\Omega} = (\mathbf{f}, \nabla \psi)_{0,\Omega} + (\rho g, \psi)_{0,\Omega}\,, \qquad \psi \in \mathrm{H}_0^1(\Omega)\,.$$

By Lax-Milgram's theorem, there exists a unique solution $p \in \mathrm{H}_0^1(\Omega)$, and the first equation in (4) yields the corresponding $\mathbf{q}$. Multiplying the second equation in (4) by ψ leads to the condition $(\mathbf{q}, \nabla \psi)_{0,\Omega} = \big(\rho(p - g), \psi\big)_{0,\Omega}$, which defines a weak divergence $\operatorname{div} \mathbf{q} \in \mathrm{L}_2(\Omega)$. Hence, $(\mathbf{q}, p) \in \mathcal{D}(A)$ is a solution of (3).

Elastic waves Elastic materials are described by the elasticity tensor $\mathbf{C}$ with $\mathbf{C}\boldsymbol{\varepsilon} \cdot \boldsymbol{\varepsilon} > c_0 \boldsymbol{\varepsilon} \cdot \boldsymbol{\varepsilon}$ for $\boldsymbol{\varepsilon} \in \mathbb{R}_{\mathrm{sym}}^{D \times D}$, where $c_0 > 0$. Here, we consider the special case of isotropic materials characterized by the Lamé parameters $\lambda \geq 0$, $\mu > 0$, and

$$\mathbf{C}\boldsymbol{\varepsilon} = 2\mu\boldsymbol{\varepsilon} + \lambda \operatorname{trace}(\boldsymbol{\varepsilon})\mathbf{I}, \qquad \mathbf{C}^{-1}\boldsymbol{\sigma} = \frac{1}{2\mu}\boldsymbol{\sigma} - \frac{\lambda}{2\mu(D\lambda + 2\mu)} \operatorname{trace}(\boldsymbol{\sigma})\mathbf{I}.$$

Elastic waves are described by the second-order system for the displacement $\boldsymbol{\varphi}$

$$\rho \partial_t^2 \boldsymbol{\varphi} + \operatorname{div} \mathbf{C}\boldsymbol{\varepsilon}(\boldsymbol{\varphi}) = \mathbf{0}\,,$$

where $\boldsymbol{\varepsilon}(\boldsymbol{\varphi}) = \operatorname{sym}(\nabla \boldsymbol{\varphi})$ denotes the strain tensor and $\rho \in \mathrm{L}_\infty(\Omega)$ is the density. Inserting the stress tensor $\boldsymbol{\sigma} = \mathbf{C}\boldsymbol{\varepsilon}(\boldsymbol{\varphi})$ and the velocity vector $\mathbf{v} = \partial_t \boldsymbol{\varphi}$, we obtain the first-order system

$$\partial_t \boldsymbol{\sigma} - \mathbf{C}\boldsymbol{\varepsilon}(\mathbf{v}) = \mathbf{0}\,, \qquad \rho \partial_t \mathbf{v} - \operatorname{div} \boldsymbol{\sigma} = \mathbf{0}$$

with $J = 5$ components for $D = 2$ and $J = 9$ for $D = 3$. We define operators

$$M(\boldsymbol{\sigma}, \mathbf{v}) = (\mathbf{C}^{-1}\boldsymbol{\sigma}, \rho\mathbf{v}), \qquad A(\boldsymbol{\sigma}, \mathbf{v}) = (-\boldsymbol{\varepsilon}(\mathbf{v}), -\operatorname{div} \boldsymbol{\sigma})$$

on the Hilbert space $V = \mathrm{L}_2(\Omega)_{\mathrm{sym}}^{D \times D} \times \mathrm{L}_2(\Omega, \mathbb{R}^D)$. Let $\partial\Omega = \partial\Omega_{\mathrm{D}} \cup \partial\Omega_{\mathrm{N}}$ be a decomposition of the boundary into Dirichlet and Neumann parts, and define the domain by

$$\mathcal{D}(A) = \big\{(\boldsymbol{\sigma}, \mathbf{v}) \in \mathrm{H}(\operatorname{div}, \Omega, \mathbb{R}^D) \times \mathrm{H}^1(\Omega, \mathbb{R}^D) \colon \boldsymbol{\sigma} = \boldsymbol{\sigma}^T,\ \boldsymbol{\sigma}\mathbf{n} = \mathbf{0} \text{ on } \partial\Omega_{\mathrm{N}}, \text{ and } \mathbf{v} = \mathbf{0} \text{ on } \partial\Omega_{\mathrm{D}}\big\}$$

where $\mathbf{n}$ is the outer unit normal vector on $\partial\Omega_{\mathrm{N}}$.

For arbitrarily chosen $(\mathbf{f}, \mathbf{g}) \in V$ we consider the elliptic problem

$$(M + A)(\boldsymbol{\sigma}, \mathbf{v}) = M(\mathbf{f}, \mathbf{g}), \tag{5}$$

which is equivalent to

$$\boldsymbol{\sigma} - \mathbf{C}\boldsymbol{\varepsilon}(\mathbf{v}) = \mathbf{f}\,, \qquad \rho\mathbf{v} - \operatorname{div} \boldsymbol{\sigma} = \rho\mathbf{g}.$$

Taking the divergence of the first equation and inserting $\operatorname{div} \boldsymbol{\sigma}$ into the second yields the variational formulation

$$(\mathbf{C}\boldsymbol{\varepsilon}(\mathbf{v}), \boldsymbol{\varepsilon}(\boldsymbol{\psi}))_{0,\Omega} + (\rho\mathbf{v}, \boldsymbol{\psi})_{0,\Omega} = -(\mathbf{f}, \boldsymbol{\varepsilon}(\boldsymbol{\psi}))_{0,\Omega} + (\rho\mathbf{g}, \boldsymbol{\psi})_{0,\Omega}$$

for all $\boldsymbol{\psi} \in \mathrm{H}^1(\Omega, \mathbb{R}^D)$ with $\boldsymbol{\psi} = \mathbf{0}$ on $\partial\Omega_{\mathrm{D}}$. Then, a unique solution $\mathbf{v} \in \mathrm{H}^1(\Omega, \mathbb{R}^D)$ with $\mathbf{v}|_{\partial\Omega_{\mathrm{D}}} = \mathbf{0}$ exists, and $(\boldsymbol{\sigma}, \mathbf{v}) = \big(\mathbf{C}\boldsymbol{\varepsilon}(\mathbf{v}) + \mathbf{f}, \mathbf{v}\big) \in \mathcal{D}(A)$ solves (5).

Electro-magnetic waves For a given permeability $\mu \in L_\infty(\Omega)$ and a permittivity $\varepsilon \in L_\infty(\Omega)$, which are uniformly positive in Ω, electro-magnetic waves are determined by the first-order system for the electric field $\mathbf{E}$ and magnetic field $\mathbf{H}$

$$\varepsilon\partial_t\mathbf{E} - \operatorname{curl}\mathbf{H} = \mathbf{0}\,, \qquad \mu\partial_t\mathbf{H} + \operatorname{curl}\mathbf{E} = \mathbf{0}\,, \qquad \operatorname{div}(\varepsilon\mathbf{E}) = 0\,, \qquad \operatorname{div}(\mu\mathbf{H}) = 0$$

with $J = 6$ components for $D = 3$. Since the last two equations will be satisfied if they are satisfied for the initial data, it is sufficient to consider only the first two equations. We thus define

$$M(\mathbf{H},\mathbf{E}) = (\mu\mathbf{H}, \varepsilon\mathbf{E}), \qquad A(\mathbf{H},\mathbf{E}) = (\operatorname{curl}\mathbf{E}, -\operatorname{curl}\mathbf{H})$$

on the Hilbert space $V = \mathrm{L}_2(\Omega)^3 \times \mathrm{L}_2(\Omega)^3$ with domain $\mathcal{D}(A) = \mathrm{H}(\operatorname{curl},\Omega) \times \mathrm{H}_0(\operatorname{curl},\Omega)$ for a material with perfectly conducting boundary. Let $(\mathbf{f},\mathbf{g}) \in V$ be arbitrary. Then the elliptic problem

$$(M + A)(\mathbf{H},\mathbf{E}) = M(\mathbf{f},\mathbf{g}), \tag{6}$$

corresponding to the system

$$\mu\mathbf{H} + \operatorname{curl}\mathbf{E} = \mu\mathbf{f}\,, \qquad \varepsilon\mathbf{E} - \operatorname{curl}\mathbf{H} = \varepsilon\mathbf{g} \tag{7}$$

can be written in variational form as

$$(\mu^{-1}\operatorname{curl}\mathbf{E}, \operatorname{curl}\boldsymbol{\psi})_{0,\Omega} + (\varepsilon\mathbf{E},\boldsymbol{\psi})_{0,\Omega} = (\mathbf{f}, \operatorname{curl}\boldsymbol{\psi})_{0,\Omega} + (\varepsilon\mathbf{g},\psi)_{0,\Omega}\,, \qquad \boldsymbol{\psi} \in \mathrm{H}_0(\operatorname{curl},\Omega).$$

This problem has a unique solution $\mathbf{E} \in \mathrm{H}_0(\operatorname{curl},\Omega)$. With the same arguments as in the previous cases, we can show that $(\mathbf{H},\mathbf{E}) = \big(\mathbf{f} - \mu^{-1}\operatorname{curl}\mathbf{E}, \mathbf{E}\big) \in \mathcal{D}(A)$ solves (6).

3 Linear systems of conservation laws

All problems discussed in the previous section can be considered as a system of linear conservation laws

$$M\partial_t\mathbf{u}(t) + \operatorname{div}\mathbf{F}(\mathbf{u}(t)) = \mathbf{0} \quad \text{for} \quad t \in [0,T]\,, \qquad \mathbf{u}(0) = \mathbf{u}_0\,, \tag{8}$$

where the linear flux is of the form $\operatorname{div}\mathbf{F}(\mathbf{u}) = \sum_{d=1}^{D} B_d\partial_d\mathbf{u}$ with symmetric matrices $B_d \in \mathbb{R}^{J\times J}$. The construction of numerical methods will be based on the formulation (8).

3.1 Discontinuous weak solutions for linear conservation laws

Since the discrete approximations will be discontinuous, we introduce the more general concept of weak solutions.

Definition 3.1 A function $\mathbf{u} \in \mathrm{L}_1((0,T)\times\Omega,\mathbb{R}^J)$ is a weak solution of (8) if

$$0 = \int_\Omega M(\mathbf{x})\mathbf{u}_0(\mathbf{x})\cdot\boldsymbol{\phi}(0,\mathbf{x})\,\mathrm{d}\mathbf{x} + \int_{(0,T)\times\Omega}\Big(M(\mathbf{x})\mathbf{u}(t,\mathbf{x})\cdot\partial_t\boldsymbol{\phi}(t,\mathbf{x}) + \mathbf{F}(\mathbf{u}(t,\mathbf{x}))\cdot\nabla\boldsymbol{\phi}(t,\mathbf{x})\Big)\,\mathrm{d}t\,\mathrm{d}\mathbf{x}$$

for all test functions with compact support $\boldsymbol{\phi} \in \mathrm{C}_0^1((-1,T)\times\Omega,\mathbb{R}^J)$.

Obviously, all smooth solutions of (8) are also weak solutions. Note that weak solutions are not unique; in particular, the definition does not include boundary conditions.

Traveling waves In the case of constant coefficients in $\Omega = \mathbb{R}^D$, special solutions can be constructed as follows. For a given unit vector $\mathbf{n} = (n_1,\dots,n_D)^T \in \mathbb{R}^D$, we have $\mathbf{n}\cdot\mathbf{F}(\mathbf{u}) = B\mathbf{u}$ with the symmetric matrix $B = \sum n_dB_d$. Then, for all eigenpairs $(\lambda,\mathbf{w}) \in \mathbb{R}\times\mathbb{R}^J$ with $B\mathbf{w} = \lambda M\mathbf{w}$ and any amplitude function $a \in \mathrm{C}^1(\mathbb{R})$, the traveling wave $\mathbf{u}(t,\mathbf{x}) = a(\mathbf{n}\cdot\mathbf{x} - \lambda t)\,\mathbf{w}$ solves (8) for $\mathbf{u}_0(\mathbf{x}) = a(\mathbf{n}\cdot\mathbf{x})\,\mathbf{w}$.

This can be extended to the case that the amplitude is discontinuous. E.g., consider the piecewise constant function

$$\mathbf{u}(t,\mathbf{x}) = \begin{cases} a_{\mathrm{L}}\mathbf{w} & \text{in } Q_{\mathrm{L}} = \big\{(t,\mathbf{x}) \in [0,T]\times\mathbb{R}^D \colon \mathbf{n}\cdot\mathbf{x} - \lambda t < 0\big\} \\ a_{\mathrm{R}}\mathbf{w} & \text{in } Q_{\mathrm{R}} = \big\{(t,\mathbf{x}) \in [0,T]\times\mathbb{R}^D \colon \mathbf{n}\cdot\mathbf{x} - \lambda t > 0\big\} \end{cases} \tag{9}$$

with $a_{\mathrm{L}}, a_{\mathrm{R}} \in \mathbb{R}$. Then, by using the Gauß theorem in $\mathbb{R} \times \mathbb{R}^D$, we observe

$$\begin{aligned}
0 &= a_{\mathrm{L}} \int_{\mathbf{n}\cdot\mathbf{x}-\lambda t=0} \big(-\lambda M + B\big)\mathbf{w} \cdot \boldsymbol{\phi}(t,\mathbf{x})\,\mathrm{d}\mathbf{a} \\
&= \int_{\partial Q_{\mathrm{L}}} \begin{pmatrix} -\lambda \\ \mathbf{n} \end{pmatrix} \cdot \begin{pmatrix} \mathbf{u}(t,\mathbf{x}) \cdot M\boldsymbol{\phi}(t,\mathbf{x}) \\ \mathbf{F}(\mathbf{u}(t,x))) \cdot \boldsymbol{\phi}(t,\mathbf{x}) \end{pmatrix} \mathrm{d}\mathbf{a} \\
&= \sqrt{1+\lambda^2} \int_{Q_{\mathrm{L}}} \begin{pmatrix} \partial_t \\ \nabla \end{pmatrix} \cdot \begin{pmatrix} \mathbf{u}(t,\mathbf{x}) \cdot M\boldsymbol{\phi}(t,\mathbf{x}) \\ \mathbf{F}(\mathbf{u}(t,x))) \cdot \boldsymbol{\phi}(t,\mathbf{x}) \end{pmatrix} \mathrm{d}t\,\mathrm{d}\mathbf{x} \\
&= \sqrt{1+\lambda^2} \int_{Q_{\mathrm{L}}} \Big(\mathbf{u}(t,\mathbf{x}) \cdot M\partial_t\boldsymbol{\phi}(t,\mathbf{x}) + \mathbf{F}(\mathbf{u}(t,\mathbf{x})) \cdot \nabla\boldsymbol{\phi}(t,\mathbf{x})\Big)\,\mathrm{d}t\,\mathrm{d}\mathbf{x}
\end{aligned}$$

for all test functions $\boldsymbol{\phi} \in \mathrm{C}_0^1((0,T)\times\Omega, \mathbb{R}^J)$. Repeating this argument with ∂Q_{R} and testing in $\mathrm{C}_0^1((-1,T)\times\Omega, \mathbb{R}^J)$ shows that (9) is a weak solution with discontinuity along the plane $\{(t,\mathbf{x})\colon \mathbf{n}\cdot\mathbf{x} - \lambda t = 0\}$ in the time-space cylinder and with discontinuous initial values $\mathbf{u}_0(\mathbf{x}) = a_{\mathrm{L}}\mathbf{w}$ in $\Omega_{\mathrm{L}} = \big\{\mathbf{x}\in\Omega\colon \mathbf{n}\cdot\mathbf{x} < 0\big\}$ and $\mathbf{u}_0(\mathbf{x}) = a_{\mathrm{R}}\mathbf{w}$ in $\Omega_{\mathrm{R}} = \big\{\mathbf{x}\in\Omega\colon \mathbf{n}\cdot\mathbf{x} > 0\big\}$.

The Riemann problem for linear conservation laws Following [27, Chap. 3.8 and 9.9], we now construct a weak solution of the Riemann problem, i.e., a piecewise constant weak solution for the discontinuous initial function

$$\mathbf{u}_0(\mathbf{x}) \quad = \quad \begin{cases} \mathbf{u}_{\mathrm{L}} & \text{in } \Omega_{\mathrm{L}} \\ \mathbf{u}_{\mathrm{R}} & \text{in } \Omega_{\mathrm{R}} \end{cases} \tag{10}$$

with $\mathbf{u}_{\mathrm{L}}, \mathbf{u}_{\mathrm{R}} \in \mathbb{R}^J$ and piecewise constant mass matrices M_{L}, M_{R} in Ω_{L} and Ω_{R}, respectively. Let $(\lambda_{j\mathrm{L}}, \mathbf{w}_{j\mathrm{L}})$ and $(\lambda_{j\mathrm{R}}, \mathbf{w}_{j\mathrm{R}})$ be the corresponding M-orthogonal eigenpairs, i.e.,

$$\begin{aligned}
B\mathbf{w}_{j\mathrm{L}} &= \lambda_{j\mathrm{L}} M_{\mathrm{L}}\mathbf{w}_{j\mathrm{L}} \qquad \text{with } \mathbf{w}_{k\mathrm{L}} \cdot M_{\mathrm{L}}\mathbf{w}_{j\mathrm{L}} = 0, \\
B\mathbf{w}_{j\mathrm{R}} &= \lambda_{j\mathrm{R}} M_{\mathrm{R}}\mathbf{w}_{j\mathrm{R}} \qquad \text{with } \mathbf{w}_{k\mathrm{R}} \cdot M_{\mathrm{R}}\mathbf{w}_{j\mathrm{R}} = 0,
\end{aligned}$$

for $j \neq k$. Then, for all coefficients $b_{j\mathrm{L}}, b_{j\mathrm{R}} \in \mathbb{R}$,

$$\mathbf{u}(t,\mathbf{x}) \quad = \quad \begin{cases} \mathbf{u}_{\mathrm{L}} + \sum_{\mathbf{x}\cdot\mathbf{n}-\lambda_{j\mathrm{L}}t>0} b_{j\mathrm{L}}\mathbf{w}_{j\mathrm{L}} & \mathbf{x}\in\Omega_{\mathrm{L}} \\ \mathbf{u}_{\mathrm{R}} + \sum_{\mathbf{x}\cdot\mathbf{n}-\lambda_{j\mathrm{R}}t<0} b_{j\mathrm{R}}\mathbf{w}_{j\mathrm{R}} & \mathbf{x}\in\Omega_{\mathrm{R}} \end{cases} \tag{11}$$

is a weak solution in $\Omega_{\mathrm{L}} \cup \Omega_{\mathrm{R}}$. In order to obtain a weak solution in $\mathbb{R}^D$, continuity of the flux on the interface is required (the Rankine-Hugoniot condition):

$$B\Big(\mathbf{u}_{\mathrm{L}} + \sum_{\lambda_{j\mathrm{L}}<0} b_{j\mathrm{L}}\mathbf{w}_{j\mathrm{L}}\Big) = B\Big(\mathbf{u}_{\mathrm{R}} + \sum_{\lambda_{j\mathrm{R}}>0} b_{j\mathrm{R}}\mathbf{w}_{j\mathrm{R}}\Big), \qquad \mathbf{x}\in\partial\Omega_{\mathrm{L}}\cap\partial\Omega_{\mathrm{R}} = \{\mathbf{x}\in\mathbb{R}^D\colon \mathbf{n}\cdot\mathbf{x} = 0\}.$$

Thus, the coefficients $b_{j\mathrm{L}}$ are determined from the jump $[\mathbf{u}_0] = \mathbf{u}_{\mathrm{R}} - \mathbf{u}_{\mathrm{L}}$ solving the equations

$$\mathbf{w}_{k\mathrm{R}} \cdot B[\mathbf{u}_0] = \mathbf{w}_{k\mathrm{R}} \cdot \sum_{\lambda_{j\mathrm{L}}<0} b_{j\mathrm{L}} B\mathbf{w}_{j\mathrm{L}} \quad \text{for} \quad \lambda_{k\mathrm{R}} < 0\,.$$

The solution of the Riemann problem defines the upwind flux on $\partial\Omega_{\mathrm{L}} \cap \partial\Omega_{\mathrm{R}}$ by

$$\mathbf{n}\cdot\mathbf{F}^*(\mathbf{u}_0) = B\Big(\mathbf{u}_{\mathrm{L}} + \sum_{\lambda_{j\mathrm{L}}<0} b_{j\mathrm{L}}\mathbf{w}_{j\mathrm{L}}\Big)\,.$$

This will be used in Section 4.3 for the construction of discontinuous discretizations.

3.2 The Riemann problem for wave equations

For the specific application to acoustic, elastic, and electro-magnetic waves we compute the eigenvectors and eigenvalues explicitly, and we provide explicit formulas for the upwind flux.

Acoustic waves For acoustic waves we have $\operatorname{div}\mathbf{F}(\mathbf{q},p) = \begin{pmatrix}\nabla p\\ \operatorname{div}\mathbf{q}\end{pmatrix}$ and thus $\mathbf{n}\cdot\mathbf{F}(\mathbf{q},p) = B\begin{pmatrix}\mathbf{q}\\ p\end{pmatrix} = \begin{pmatrix}p\mathbf{n}\\ \mathbf{q}\cdot\mathbf{n}\end{pmatrix}$. Let $c = \frac{1}{\sqrt{\rho}}$ be the velocity of sound. Then $\mathbf{w}_\pm = \begin{pmatrix}\mathbf{n}\\ \pm c\end{pmatrix}$ are eigenvectors with $B\mathbf{w}_\pm = \pm cM\mathbf{w}_\pm$.

The solution (11) of the Riemann problem with piecewise constant mass matrices M_{L}, M_{R} is of the form

$$\mathbf{u}(t,\mathbf{x}) \;=\; \begin{cases} \begin{pmatrix}\mathbf{q}_{\mathrm{L}}\\ p_{\mathrm{L}}\end{pmatrix} & c_{\mathrm{L}}t+\mathbf{x}\cdot\mathbf{n}<0\\ \begin{pmatrix}\mathbf{q}_{\mathrm{L}}\\ p_{\mathrm{L}}\end{pmatrix} + b_{\mathrm{L}}\begin{pmatrix}\mathbf{n}\\ -c_{\mathrm{L}}\end{pmatrix} & c_{\mathrm{L}}t+\mathbf{x}\cdot\mathbf{n}>0 \text{ and } \mathbf{x}\cdot\mathbf{n}<0\\ \begin{pmatrix}\mathbf{q}_{\mathrm{R}}\\ p_{\mathrm{R}}\end{pmatrix} + b_{\mathrm{R}}\begin{pmatrix}\mathbf{n}\\ c_{\mathrm{R}}\end{pmatrix} & -c_{\mathrm{R}}t+\mathbf{x}\cdot\mathbf{n}<0 \text{ and } \mathbf{x}\cdot\mathbf{n}>0\\ \begin{pmatrix}\mathbf{q}_{\mathrm{R}}\\ p_{\mathrm{R}}\end{pmatrix} & -c_{\mathrm{R}}t+\mathbf{x}\cdot\mathbf{n}>0 \end{cases}$$

with the continuity constraint $B\left(\begin{pmatrix}\mathbf{q}_{\mathrm{L}}\\ p_{\mathrm{L}}\end{pmatrix} + b_{\mathrm{L}}\begin{pmatrix}\mathbf{n}\\ -c_{\mathrm{L}}\end{pmatrix}\right) = B\left(\begin{pmatrix}\mathbf{q}_{\mathrm{R}}\\ p_{\mathrm{R}}\end{pmatrix} + b_{\mathrm{R}}\begin{pmatrix}\mathbf{n}\\ c_{\mathrm{R}}\end{pmatrix}\right)$ for the flux at the interface $\partial\Omega_{\mathrm{L}}\cap\partial\Omega_{\mathrm{R}}$. Multiplying with $\begin{pmatrix}\mathbf{n}\\ -c_{\mathrm{R}}\end{pmatrix}$ shows that b_{L} can be computed from $[\mathbf{q}] = \mathbf{q}_{\mathrm{R}} - \mathbf{q}_{\mathrm{L}}$ and $[p] = p_{\mathrm{R}} - p_{\mathrm{L}}$ by

$$-b_{\mathrm{L}}(c_{\mathrm{L}}+c_{\mathrm{R}}) \;=\; b_{\mathrm{L}}B\begin{pmatrix}\mathbf{n}\\ -c_{\mathrm{L}}\end{pmatrix}\cdot\begin{pmatrix}\mathbf{n}\\ -c_{\mathrm{R}}\end{pmatrix} = B\left(\begin{pmatrix}\mathbf{q}_{\mathrm{R}}\\ p_{\mathrm{R}}\end{pmatrix} - \begin{pmatrix}\mathbf{q}_{\mathrm{L}}\\ p_{\mathrm{L}}\end{pmatrix}\right)\cdot\begin{pmatrix}\mathbf{n}\\ -c_{\mathrm{R}}\end{pmatrix} = [p] - c_{\mathrm{R}}[\mathbf{q}]\cdot\mathbf{n}\,.$$

This finally yields the expression for the upwind flux

$$\begin{aligned}\mathbf{n}\cdot\mathbf{F}^*(\mathbf{u}_0) &= B\left(\begin{pmatrix}\mathbf{q}_{\mathrm{L}}\\ p_{\mathrm{L}}\end{pmatrix} - \frac{[p]-c_{\mathrm{R}}[\mathbf{q}]\cdot\mathbf{n}}{c_{\mathrm{L}}+c_{\mathrm{R}}}\begin{pmatrix}\mathbf{n}\\ -c_{\mathrm{L}}\end{pmatrix}\right) = B\begin{pmatrix}\mathbf{q}_{\mathrm{L}}\\ p_{\mathrm{L}}\end{pmatrix} - \frac{[p]-c_{\mathrm{R}}[\mathbf{q}]\cdot\mathbf{n}}{c_{\mathrm{L}}+c_{\mathrm{R}}}\begin{pmatrix}-c_{\mathrm{L}}\mathbf{n}\\ 1\end{pmatrix}\\ &= B\begin{pmatrix}\mathbf{q}_{\mathrm{L}}\\ p_{\mathrm{L}}\end{pmatrix} + \frac{c_{\mathrm{L}}}{c_{\mathrm{L}}+c_{\mathrm{R}}}\begin{pmatrix}[p]\mathbf{n}\\ 0\end{pmatrix} - \frac{1}{c_{\mathrm{L}}+c_{\mathrm{R}}}\begin{pmatrix}\mathbf{0}\\ [p]\end{pmatrix} - \frac{c_{\mathrm{L}}c_{\mathrm{R}}}{c_{\mathrm{L}}+c_{\mathrm{R}}}\begin{pmatrix}([\mathbf{q}]\cdot\mathbf{n})\mathbf{n}\\ 0\end{pmatrix} + \frac{c_{\mathrm{R}}}{c_{\mathrm{L}}+c_{\mathrm{R}}}\begin{pmatrix}\mathbf{0}\\ [\mathbf{q}]\cdot\mathbf{n}\end{pmatrix}.\end{aligned}$$

Elastic waves In the elastic case, we have $\operatorname{div}\mathbf{F}(\boldsymbol{\sigma},\mathbf{v}) = -\begin{pmatrix}\boldsymbol{\varepsilon}(\mathbf{v})\\ \operatorname{div}\boldsymbol{\sigma}\end{pmatrix}$ and $\mathbf{n}\cdot\mathbf{F}(\boldsymbol{\sigma},\mathbf{v}) = -\begin{pmatrix}\frac{1}{2}(\mathbf{n}\otimes\mathbf{v}+\mathbf{v}\otimes\mathbf{n})\\ \boldsymbol{\sigma}\mathbf{n}\end{pmatrix}$. By $c_{\mathrm{P}} = \sqrt{\frac{2\mu/3+\lambda}{\rho}}$ we denote the velocity of pressure waves, and by $c_{\mathrm{S}} = \sqrt{\frac{\mu}{\rho}}$ the velocity of shear waves. The eigenvectors are of the form $\begin{pmatrix}2\mu\mathbf{n}\otimes\mathbf{n}+\lambda\mathbf{I}\\ \pm c_{\mathrm{P}}\mathbf{n}\end{pmatrix}$ and $\begin{pmatrix}\mu\boldsymbol{\tau}\otimes\mathbf{n}+\mu\mathbf{n}\otimes\boldsymbol{\tau}\\ \pm c_{\mathrm{S}}\boldsymbol{\tau}\end{pmatrix}$, where $\boldsymbol{\tau}$ is a unit tangent vector, i.e., $\boldsymbol{\tau}\cdot\mathbf{n}=0$.

For piecewise constant mass matrices M_{L}, M_{R} and $D=2$ the Riemann solution is of the form

$$\mathbf{u}(t,\mathbf{x}) = \begin{cases} \begin{pmatrix}\boldsymbol{\sigma}_{\mathrm{L}}\\ \mathbf{v}_{\mathrm{L}}\end{pmatrix} & c_{\mathrm{PL}}t+\mathbf{x}\cdot\mathbf{n}<0\\ \begin{pmatrix}\boldsymbol{\sigma}_{\mathrm{L}}\\ \mathbf{v}_{\mathrm{L}}\end{pmatrix} + a_{\mathrm{L}}\begin{pmatrix}2\mu_{\mathrm{L}}\mathbf{n}\otimes\mathbf{n}+\lambda_{\mathrm{L}}\mathbf{I}\\ c_{\mathrm{PL}}\mathbf{n}\end{pmatrix} & c_{\mathrm{PL}}t+\mathbf{x}\cdot\mathbf{n}>0 \text{ and } c_{\mathrm{SL}}t+\mathbf{x}\cdot\mathbf{n}<0\\ \begin{pmatrix}\boldsymbol{\sigma}_{\mathrm{L}}\\ \mathbf{v}_{\mathrm{L}}\end{pmatrix} + a_{\mathrm{L}}\begin{pmatrix}2\mu_{\mathrm{L}}\mathbf{n}\otimes\mathbf{n}+\lambda_{\mathrm{L}}\mathbf{I}\\ -c_{\mathrm{PL}}\mathbf{n}\end{pmatrix} + b_{\mathrm{L}}\begin{pmatrix}\mu_{\mathrm{L}}\boldsymbol{\tau}\otimes\mathbf{n}+\mu_{\mathrm{L}}\mathbf{n}\otimes\boldsymbol{\tau}\\ -c_{\mathrm{SL}}\boldsymbol{\tau}\end{pmatrix} & c_{\mathrm{SL}}t+\mathbf{x}\cdot\mathbf{n}>0 \text{ and } \mathbf{x}\cdot\mathbf{n}<0\\ \begin{pmatrix}\boldsymbol{\sigma}_{\mathrm{R}}\\ \mathbf{v}_{\mathrm{R}}\end{pmatrix} + a_{\mathrm{R}}\begin{pmatrix}2\mu_{\mathrm{R}}\mathbf{n}\otimes\mathbf{n}+\lambda_{\mathrm{R}}\mathbf{I}\\ c_{\mathrm{PR}}\mathbf{n}\end{pmatrix} + b_{\mathrm{R}}\begin{pmatrix}\mu_{\mathrm{R}}\boldsymbol{\tau}\otimes\mathbf{n}+\mu_{\mathrm{R}}\mathbf{n}\otimes\boldsymbol{\tau}\\ c_{\mathrm{SR}}\boldsymbol{\tau}\end{pmatrix} & -c_{\mathrm{SR}}t+\mathbf{x}\cdot\mathbf{n}<0 \text{ and } \mathbf{x}\cdot\mathbf{n}>0\\ \begin{pmatrix}\boldsymbol{\sigma}_{\mathrm{R}}\\ \mathbf{v}_{\mathrm{R}}\end{pmatrix} + a_{\mathrm{R}}\begin{pmatrix}2\mu_{\mathrm{R}}\mathbf{n}\otimes\mathbf{n}+\lambda_{\mathrm{R}}\mathbf{I}\\ -c_{\mathrm{PR}}\mathbf{n}\end{pmatrix} & -c_{\mathrm{SR}}t+\mathbf{x}\cdot\mathbf{n}>0 \text{ and } -c_{\mathrm{PR}}t+\mathbf{x}\cdot\mathbf{n}<0\\ \begin{pmatrix}\boldsymbol{\sigma}_{\mathrm{R}}\\ \mathbf{v}_{\mathrm{R}}\end{pmatrix} & -c_{\mathrm{PR}}t+\mathbf{x}\cdot\mathbf{n}>0 \end{cases}$$

with the continuity constraint for the flux at the interface $\partial\Omega_{\rm L} \cap \partial\Omega_{\rm R}$

$$B\left(\begin{pmatrix}\boldsymbol{\sigma}_{\rm L}\\ \mathbf{v}_{\rm L}\end{pmatrix} + a_{\rm L}\begin{pmatrix}2\mu_{\rm L}\mathbf{n}\otimes\mathbf{n}+\lambda_{\rm L}\mathbf{I}\\ c_{\rm PL}\mathbf{n}\end{pmatrix} + b_{\rm L}\begin{pmatrix}\mu_{\rm L}\boldsymbol{\tau}\otimes\mathbf{n}+\mu_{\rm L}\mathbf{n}\otimes\boldsymbol{\tau}\\ c_{\rm SL}\boldsymbol{\tau}\end{pmatrix}\right)$$
$$= B\left(\begin{pmatrix}\boldsymbol{\sigma}_{\rm R}\\ \mathbf{v}_{\rm R}\end{pmatrix} + a_{\rm R}\begin{pmatrix}2\mu_{\rm R}\mathbf{n}\otimes\mathbf{n}+\lambda_{\rm R}\mathbf{I}\\ -c_{\rm PR}\mathbf{n}\end{pmatrix} + b_{\rm R}\begin{pmatrix}\mu_{\rm R}\boldsymbol{\tau}\otimes\mathbf{n}+\mu_{\rm R}\mathbf{n}\otimes\boldsymbol{\tau}\\ -c_{\rm SR}\boldsymbol{\tau}\end{pmatrix}\right).$$

This yields for $[\boldsymbol{\sigma}] = \boldsymbol{\sigma}_{\rm R} - \boldsymbol{\sigma}_{\rm L}$ and $[\mathbf{v}] = \mathbf{v}_{\rm R} - \mathbf{v}_{\rm L}$

$$\begin{aligned}
-a_{\rm L}(c_{\rm PL}(2\mu_{\rm R}+\lambda_{\rm R}) + (2\mu_{\rm L}+\lambda_{\rm L})c_{\rm PR}) &= B\begin{pmatrix}[\boldsymbol{\sigma}]\\ [\mathbf{v}]\end{pmatrix}\cdot\begin{pmatrix}2\mu_{\rm R}\mathbf{n}\otimes\mathbf{n}+\lambda_{\rm R}\mathbf{I}\\ c_{\rm PR}\mathbf{n}\end{pmatrix} = -(2\mu_{\rm R}+\lambda_{\rm R})[\mathbf{v}]\cdot\mathbf{n} - c_{\rm PR}([\boldsymbol{\sigma}]\mathbf{n})\cdot\mathbf{n}\,,\\
-b_{\rm L}(c_{\rm SL}\mu_{\rm R} + \mu_{\rm L}c_{\rm SR}) &= B\begin{pmatrix}[\boldsymbol{\sigma}]\\ [\mathbf{v}]\end{pmatrix}\cdot\begin{pmatrix}\mu_{\rm R}\boldsymbol{\tau}\otimes\mathbf{n}+\mu_{\rm R}\mathbf{n}\otimes\boldsymbol{\tau}\\ c_{\rm SR}\boldsymbol{\tau}\end{pmatrix} = -\mu_{\rm R}[\mathbf{v}]\cdot\boldsymbol{\tau} - c_{\rm SR}([\boldsymbol{\sigma}]\mathbf{n})\cdot\boldsymbol{\tau}\,,
\end{aligned}$$

and finally the upwind flux (see also [24] for the case $M_{\rm R} = M_{\rm L}$)

$$\begin{aligned}
\mathbf{n}\cdot\mathbf{F}^*(\mathbf{u}_0) &= \begin{pmatrix}\boldsymbol{\sigma}_{\rm L}\\ \mathbf{v}_{\rm L}\end{pmatrix} + \frac{(2\mu_{\rm R}+\lambda_{\rm R})[\mathbf{v}]\cdot\mathbf{n} + c_{\rm PR}([\boldsymbol{\sigma}]\mathbf{n})\cdot\mathbf{n}}{c_{\rm PL}(2\mu_{\rm R}+\lambda_{\rm R}) + (2\mu_{\rm L}+\lambda_{\rm L})c_{\rm PR}} B\begin{pmatrix}2\mu_{\rm L}\mathbf{n}\otimes\mathbf{n}+\lambda_{\rm L}\mathbf{I}\\ c_{\rm PL}\mathbf{n}\end{pmatrix}\\
&\quad + \frac{\mu_{\rm R}[\mathbf{v}]\cdot\boldsymbol{\tau} + c_{\rm SR}([\boldsymbol{\sigma}]\mathbf{n})\cdot\boldsymbol{\tau}}{c_{\rm SL}\mu_{\rm R} + \mu_{\rm L}c_{\rm SR}} B\begin{pmatrix}\mu_{\rm L}\boldsymbol{\tau}\otimes\mathbf{n}+\mu_{\rm L}\mathbf{n}\otimes\boldsymbol{\tau}\\ c_{\rm SL}\boldsymbol{\tau}\end{pmatrix}\\
&= \begin{pmatrix}\boldsymbol{\sigma}_{\rm L}\\ \mathbf{v}_{\rm L}\end{pmatrix} - \frac{(2\mu_{\rm R}+\lambda_{\rm R})[\mathbf{v}]\cdot\mathbf{n}}{c_{\rm PL}(2\mu_{\rm R}+\lambda_{\rm R}) + (2\mu_{\rm L}+\lambda_{\rm L})c_{\rm PR}}\begin{pmatrix}c_{\rm PL}\mathbf{n}\otimes\mathbf{n}\\ (2\mu_{\rm L}+\lambda_{\rm L})\mathbf{n}\end{pmatrix}\\
&\quad - \frac{\mu_{\rm R}[\mathbf{v}]\cdot\boldsymbol{\tau}}{c_{\rm SL}\mu_{\rm R}+\mu_{\rm L}c_{\rm SR}}\begin{pmatrix}\frac{1}{2}c_{\rm SL}(\boldsymbol{\tau}\otimes\mathbf{n}+\mathbf{n}\otimes\boldsymbol{\tau})\\ \mu_{\rm L}\boldsymbol{\tau}\end{pmatrix}\\
&\quad - \frac{c_{\rm PR}([\boldsymbol{\sigma}]\mathbf{n})\cdot\mathbf{n}}{c_{\rm PL}(2\mu_{\rm R}+\lambda_{\rm R}) + (2\mu_{\rm L}+\lambda_{\rm L})c_{\rm PR}}\begin{pmatrix}c_{\rm PL}\mathbf{n}\otimes\mathbf{n}\\ (2\mu_{\rm L}+\lambda_{\rm L})\mathbf{n}\end{pmatrix}\\
&\quad - \frac{c_{\rm SR}([\boldsymbol{\sigma}]\mathbf{n})\cdot\boldsymbol{\tau}}{c_{\rm SL}\mu_{\rm R}+\mu_{\rm L}c_{\rm SR}}\begin{pmatrix}\frac{1}{2}c_{\rm SL}(\boldsymbol{\tau}\otimes\mathbf{n}+\mathbf{n}\otimes\boldsymbol{\tau})\\ \mu_{\rm L}\boldsymbol{\tau}\end{pmatrix}.
\end{aligned}$$

Electro-magnetic waves Here we have $\operatorname{div}\mathbf{F}(\mathbf{H},\mathbf{E}) = \begin{pmatrix}\operatorname{curl}\mathbf{E}\\ -\operatorname{curl}\mathbf{H}\end{pmatrix}$ and thus $\mathbf{n}\cdot\mathbf{F}(\mathbf{H},\mathbf{E}) = B\begin{pmatrix}\mathbf{H}\\ \mathbf{E}\end{pmatrix} = \begin{pmatrix}\mathbf{n}\times\mathbf{E}\\ -\mathbf{n}\times\mathbf{H}\end{pmatrix}$. By $c = \frac{1}{\sqrt{\varepsilon\mu}}$ we denote the speed of light. Then $\begin{pmatrix}\sqrt{\varepsilon}\mathbf{n}\times\boldsymbol{\tau}\\ \pm\sqrt{\mu}\boldsymbol{\tau}\end{pmatrix}$ and $\begin{pmatrix}\mp\sqrt{\varepsilon}\boldsymbol{\tau}\\ \sqrt{\mu}\mathbf{n}\times\boldsymbol{\tau}\end{pmatrix}$ are the corresponding eigenvectors, where again $\boldsymbol{\tau}$ is a unit tangent vector. For piecewise constant mass matrices $M_{\rm L}$, $M_{\rm R}$ the Riemann solution is

$$\mathbf{u}(t,\mathbf{x}) = \begin{cases}
\begin{pmatrix}\mathbf{H}_{\rm L}\\ \mathbf{E}_{\rm L}\end{pmatrix} & c_{\rm L}t + \mathbf{x}\cdot\mathbf{n} < 0\\
\begin{pmatrix}\mathbf{H}_{\rm L}\\ \mathbf{E}_{\rm L}\end{pmatrix} + a_{\rm L}\begin{pmatrix}\sqrt{\varepsilon_{\rm L}}\boldsymbol{\tau}\\ \sqrt{\mu_{\rm L}}\mathbf{n}\times\boldsymbol{\tau}\end{pmatrix} + b_{\rm L}\begin{pmatrix}\sqrt{\varepsilon_{\rm L}}\mathbf{n}\times\boldsymbol{\tau}\\ -\sqrt{\mu_{\rm L}}\boldsymbol{\tau}\end{pmatrix} & c_{\rm L}t + \mathbf{x}\cdot\mathbf{n} > 0 \text{ and } \mathbf{x}\cdot\mathbf{n} < 0\\
\begin{pmatrix}\mathbf{H}_{\rm R}\\ \mathbf{E}_{\rm R}\end{pmatrix} + a_{\rm R}\begin{pmatrix}-\sqrt{\varepsilon_{\rm R}}\boldsymbol{\tau}\\ \sqrt{\mu_{\rm R}}\mathbf{n}\times\boldsymbol{\tau}\end{pmatrix} + b_{\rm R}\begin{pmatrix}\sqrt{\varepsilon_{\rm R}}\mathbf{n}\times\boldsymbol{\tau}\\ \sqrt{\mu_{\rm R}}\boldsymbol{\tau}\end{pmatrix} & -c_{\rm R}t + \mathbf{x}\cdot\mathbf{n} < 0 \text{ and } \mathbf{x}\cdot\mathbf{n} > 0\\
\begin{pmatrix}\mathbf{H}_{\rm R}\\ \mathbf{E}_{\rm R}\end{pmatrix} & -c_{\rm R}t + \mathbf{x}\cdot\mathbf{n} > 0
\end{cases}$$

with the continuity constraint for the flux at the interface $\partial\Omega_{\rm L} \cap \partial\Omega_{\rm R}$

$$B\left(\begin{pmatrix}\mathbf{H}_{\rm L}\\ \mathbf{E}_{\rm L}\end{pmatrix} + a_{\rm L}\begin{pmatrix}\sqrt{\varepsilon_{\rm L}}\boldsymbol{\tau}\\ \sqrt{\mu_{\rm L}}\mathbf{n}\times\boldsymbol{\tau}\end{pmatrix} + b_{\rm L}\begin{pmatrix}\sqrt{\varepsilon_{\rm L}}\mathbf{n}\times\boldsymbol{\tau}\\ -\sqrt{\mu_{\rm L}}\boldsymbol{\tau}\end{pmatrix}\right) = B\left(\begin{pmatrix}\mathbf{H}_{\rm R}\\ \mathbf{E}_{\rm R}\end{pmatrix} + a_{\rm R}\begin{pmatrix}-\sqrt{\varepsilon_{\rm R}}\boldsymbol{\tau}\\ \sqrt{\mu_{\rm R}}\mathbf{n}\times\boldsymbol{\tau}\end{pmatrix} + b_{\rm R}\begin{pmatrix}\sqrt{\varepsilon_{\rm R}}\mathbf{n}\times\boldsymbol{\tau}\\ \sqrt{\mu_{\rm R}}\boldsymbol{\tau}\end{pmatrix}\right).$$

For the jumps $[\mathbf{H}] = \mathbf{H}_{\rm R} - \mathbf{H}_{\rm L}$ and $[\mathbf{E}] = \mathbf{E}_{\rm R} - \mathbf{E}_{\rm L}$ this yields

$$\begin{aligned}
-a_{\rm L}(\sqrt{\varepsilon_{\rm L}\mu_{\rm R}} + \sqrt{\mu_{\rm L}\varepsilon_{\rm R}}) &= B\begin{pmatrix}[\mathbf{H}]\\ [\mathbf{E}]\end{pmatrix}\cdot\begin{pmatrix}\sqrt{\varepsilon_{\rm R}}\boldsymbol{\tau}\\ \sqrt{\mu_{\rm R}}\mathbf{n}\times\boldsymbol{\tau}\end{pmatrix} = \sqrt{\varepsilon_{\rm R}}(\mathbf{n}\times[\mathbf{E}])\cdot\boldsymbol{\tau} - \sqrt{\mu_{\rm R}}(\mathbf{n}\times[\mathbf{H}])\cdot(\mathbf{n}\times\boldsymbol{\tau})\,,\\
-b_{\rm L}(\sqrt{\varepsilon_{\rm L}\mu_{\rm R}} + \sqrt{\mu_{\rm L}\varepsilon_{\rm R}}) &= B\begin{pmatrix}[\mathbf{H}]\\ [\mathbf{E}]\end{pmatrix}\cdot\begin{pmatrix}\sqrt{\varepsilon_{\rm R}}\mathbf{n}\times\boldsymbol{\tau}\\ -\sqrt{\mu_{\rm R}}\boldsymbol{\tau}\end{pmatrix} = \sqrt{\varepsilon_{\rm R}}(\mathbf{n}\times[\mathbf{E}])\cdot(\mathbf{n}\times\boldsymbol{\tau}) + \sqrt{\mu_{\rm R}}(\mathbf{n}\times[\mathbf{H}])\cdot\boldsymbol{\tau}
\end{aligned}$$

and thus the expression for the upwind flux (cf. [19])

$$\begin{aligned}\mathbf{n}\cdot\mathbf{F}^*(\mathbf{u}_0) &= B\begin{pmatrix}\mathbf{H}_\mathrm{L}\\ \mathbf{E}_\mathrm{L}\end{pmatrix} - \frac{\sqrt{\varepsilon_\mathrm{R}}(\mathbf{n}\times[\mathbf{E}])\cdot\boldsymbol{\tau} - \sqrt{\mu_\mathrm{R}}(\mathbf{n}\times[\mathbf{H}])\cdot(\mathbf{n}\times\boldsymbol{\tau})}{\sqrt{\varepsilon_\mathrm{L}\mu_\mathrm{R}}+\sqrt{\mu_\mathrm{L}\varepsilon_\mathrm{R}}} B\begin{pmatrix}\sqrt{\varepsilon_\mathrm{L}}\boldsymbol{\tau}\\ \sqrt{\mu_\mathrm{L}}\mathbf{n}\times\boldsymbol{\tau}\end{pmatrix}\\ &\qquad - \frac{\sqrt{\varepsilon_\mathrm{R}}(\mathbf{n}\times[\mathbf{E}])\cdot(\mathbf{n}\times\boldsymbol{\tau}) + \sqrt{\mu_\mathrm{R}}(\mathbf{n}\times[\mathbf{H}])\cdot\boldsymbol{\tau}}{\sqrt{\varepsilon_\mathrm{L}\mu_\mathrm{R}}+\sqrt{\mu_\mathrm{L}\varepsilon_\mathrm{R}}} B\begin{pmatrix}\sqrt{\varepsilon_\mathrm{L}}\mathbf{n}\times\boldsymbol{\tau}\\ -\sqrt{\mu_\mathrm{L}}\boldsymbol{\tau}\end{pmatrix}\\ &= B\begin{pmatrix}\mathbf{H}_\mathrm{L}\\ \mathbf{E}_\mathrm{L}\end{pmatrix} + \frac{\varepsilon_\mathrm{R}c_\mathrm{R}}{\varepsilon_\mathrm{L}c_\mathrm{L}+\varepsilon_\mathrm{R}c_\mathrm{R}}\begin{pmatrix}\mathbf{n}\times[\mathbf{E}]\\ \mathbf{0}\end{pmatrix} + \frac{1}{\mu_\mathrm{L}c_\mathrm{L}+\mu_\mathrm{R}c_\mathrm{R}}\begin{pmatrix}\mathbf{0}\\ \mathbf{n}\times(\mathbf{n}\times[\mathbf{E}])\end{pmatrix}\\ &\qquad - \frac{\mu_\mathrm{R}c_\mathrm{R}}{\mu_\mathrm{L}c_\mathrm{L}+\mu_\mathrm{R}c_\mathrm{R}}\begin{pmatrix}\mathbf{0}\\ \mathbf{n}\times[\mathbf{H}]\end{pmatrix} + \frac{1}{\varepsilon_\mathrm{L}c_\mathrm{L}+\varepsilon_\mathrm{R}c_\mathrm{R}}\begin{pmatrix}\mathbf{n}\times(\mathbf{n}\times[\mathbf{H}])\\ \mathbf{0}\end{pmatrix}.\end{aligned}$$

We are now in the position to construct the discrete operators for the specific applications.

4 A discontinuous Galerkin approximation for the wave equations

In this section we consider the discrete evolution equation

$$M\partial_t\mathbf{u}_h(t) + A_h\mathbf{u}_h(t) = 0\,, \qquad t\in[0,T] \tag{12}$$

in a subspace $V_h\subset V$ associated to the mesh size h. We are interested in the semi-discrete convergence to the solution of (1), where the discrete operator $A_h\in\mathcal{L}(V_h,V_h)$ is constructed from a discontinuous Galerkin discretization with upwind flux obtained from local solutions of Riemann problems of the previous section.

4.1 The discrete operator for linear systems of conservation laws

Here we assume that $\Omega\subset\mathbb{R}^D$, $D=2,3$ is a bounded polyhedral Lipschitz domain decomposed into a finite number of open elements $K\subset\Omega$ such that $\bar\Omega=\bigcup\bar K$. Let $\mathcal{F}_K$ be the set of faces of K, and for $f\in\mathcal{F}_K$ let K_f be the neighboring cell such that $f=\partial K\cap\partial K_f$, and let $\mathbf{n}_{K,f}$ be the outer unit normal vector on $f\subset\partial K$. The outer unit normal vector field on $\partial\Omega$ is denoted by $\mathbf{n}$. Furthermore, we assume that the mass operator M is constant in K, i.e., $M(\mathbf{x})=M_K$, $\mathbf{x}\in K$, is a symmetric positive definite matrix. Finally, we define $V_K=\mathrm{L}_2(K,\mathbb{R}^J)$.

Integration by parts gives for locally smooth test functions

$$(A\mathbf{v},\boldsymbol{\phi}_K)_{0,K} = -(\mathbf{F}(\mathbf{v}),\nabla\boldsymbol{\phi}_K)_{0,K} + \sum_{f\in\mathcal{F}_K}(\mathbf{n}_{K,f}\cdot\mathbf{F}(\mathbf{v}),\boldsymbol{\phi}_K)_{0,f}\,.$$

This formulation is now the basis for the discretization. We fix a polynomial degree p, and we define the local spaces $V_{K,h}=\mathbb{P}_p(K)^J$ and the global discontinuous Galerkin space $V_h=\{\mathbf{v}_h\in\mathrm{L}_2(\Omega,\mathbb{R}^J)\colon \mathbf{v}_h|_K\in V_{K,h}\}$. For $\mathbf{v}_h\in V_h$ we use $\mathbf{v}_{K,h}=\mathbf{v}_h|_K\in V_{K,h}$ for the restriction to K.

For a given function $\mathbf{v}_h\in V_h$ we define the discrete linear operator $A_h\in\mathcal{L}(V_h,V_h)$ by

$$(A_h\mathbf{v}_h,\boldsymbol{\phi}_{K,h})_{0,K} = -(\mathbf{F}(\mathbf{v}_{K,h}),\nabla\boldsymbol{\phi}_{K,h})_{0,K} + \sum_{f\in\mathcal{F}_K}(\mathbf{n}_{K,f}\cdot\mathbf{F}^*_{K,f}(\mathbf{v}_h),\boldsymbol{\phi}_{K,h})_{0,f}\,,$$

where $\mathbf{n}_{K,f}\cdot\mathbf{F}^*_{K,f}(\mathbf{v}_h)$ is the upwind flux obtain from the solution of the Riemann problem with initial values $\mathbf{u}_\mathrm{L}=\mathbf{v}_{K,h}(\mathbf{x})$ and $\mathbf{u}_\mathrm{R}=\mathbf{v}_{K_f,h}(\mathbf{x})$ for $\mathbf{x}\in f=\partial K\cap\partial K_f$ on inner faces $f\subset\Omega$. For boundary faces $f=\partial K\cap\partial\Omega$ we define $\mathbf{u}_\mathrm{R}$ depending on the boundary conditions and the specific application. Again using integration by parts, we obtain

$$(A_h\mathbf{v}_h,\boldsymbol{\phi}_{K,h})_{0,K} = (\operatorname{div}\mathbf{F}(\mathbf{v}_{K,h}),\boldsymbol{\phi}_{K,h})_{0,K} + \sum_{f\in\mathcal{F}_K}\big(\mathbf{n}_{K,f}\cdot(\mathbf{F}^*_{K,f}(\mathbf{v}_h)-\mathbf{F}(\mathbf{v}_{K,h})),\boldsymbol{\phi}_{K,h}\big)_{0,f}\,. \tag{13}$$

Note that the term $\mathbf{n}_{K,f}\cdot(\mathbf{F}^*_{K,f}(\mathbf{v}_h)-\mathbf{F}(\mathbf{v}_{K,h}))$ only depends on $[\mathbf{v}_h]_{K,f}=\mathbf{v}_{K_f,h}-\mathbf{v}_{K,h}$. Moreover, this definition includes finite volume discretizations with $p=0$, where the discrete operator is defined only by the flux terms on the faces $\mathcal{F}_K$.

Since we use the upwind flux from the solution of the Riemann problem, we observe for $\mathbf{v}\in\mathcal{D}(A)$ and $\mathbf{v}_h\in V_h$

$$(\operatorname{div}\mathbf{F}(\mathbf{v}),\mathbf{v}_h)_{0,\Omega} + \sum_K\Big((\operatorname{div}\mathbf{F}(\mathbf{v}_{K,h}),\mathbf{v})_{0,K} + \sum_{f\in\mathcal{F}_K}(\mathbf{n}_{K,f}\cdot(\mathbf{F}^*_{K,f}(\mathbf{v}_h)-\mathbf{F}(\mathbf{v}_{K,h})),\mathbf{v})_{0,f}\Big) = 0\,. \tag{14}$$

Together with the formulation (13) this will be the basis for the error analysis below.

4.2 Stability, consistency, and semi-discrete convergence

Let $\Pi_{K,h}\colon V_K \longrightarrow V_{K,h}$ be the local L_2 orthogonal projection. Then, we have for $1 \le q \le p+1$

$$\|\mathbf{v} - \Pi_{K,h}\mathbf{v}\|_{0,K} \le Ch^q \|\mathbf{v}\|_{q,K}\,, \qquad \mathbf{v} \in \mathrm{H}^q(K, \mathbb{R}^J)\,,$$

which gives $\|\mathbf{v} - \Pi_{K,h}\mathbf{v}\|_{0,f} \le Ch^{q-1/2}\|\mathbf{v}\|_{q,K}$ and thus, with some $C_{\mathrm{R}} > 0$,

$$\frac{1}{2}\sum_K \sum_{f\in\mathcal{F}_K} \|\mathbf{v} - \Pi_{K,h}\mathbf{v}\|_{0,f}^2 \le C_{\mathrm{R}} h^{2q-1}\|\mathbf{v}\|_{q,\Omega}^2\,, \qquad \mathbf{v} \in \mathrm{H}^q(\Omega, \mathbb{R}^J)\,. \tag{15}$$

Theorem 4.1 *Let $\mathbf{u} \in \mathrm{C}^1([0,T], \mathcal{D}(A))$ be a solution of the evolution equation* (1)*, and let $\mathbf{u}_h \in \mathrm{C}^1([0,T], V_h)$ be a solution of the discretization* (12)*. We assume that the solution has the regularity $\mathbf{u} \in \mathrm{L}_2((0,T), \mathrm{H}^q(\Omega, \mathbb{R}^J))$ for some $1 \le q \le p+1$. For the discrete operator A_h we assume that a constant $C_A > 0$ exists such that*

$$\frac{1}{2}\sum_K \sum_{f\in\mathcal{F}_K} \left\|\mathbf{n}_{K,f} \cdot \left(\mathbf{F}^*_{K,f}(\mathbf{v}_h) - \mathbf{F}(\mathbf{v}_{K,h})\right)\right\|_{0,f}^2 \le C_{\mathrm{A}}\,(A_h\mathbf{v}_h, \mathbf{v}_h)_{0,\Omega}\,, \qquad \mathbf{v}_h \in V_h\,. \tag{16}$$

Then, the following a priori estimate holds

$$\|\mathbf{u} - \mathbf{u}_h\|^2_{\mathrm{L}_2([0,T],V)} \le 2TC_{\mathrm{A}}C_{\mathrm{R}}h^{2q-1}\,\|\mathbf{u}\|^2_{\mathrm{L}_2([0,T],\mathrm{H}^q(\Omega,\mathbb{R}^J))} + T\,\|\mathbf{u}(0) - \mathbf{u}_h(0)\|_V^2\,.$$

For consistent initial values this implies convergence to the solution in L_2 of order $h^{q-1/2}$ and thus also asymptotic energy conservation. This proof follows the ideas for the finite volume analysis in [38].

P r o o f. Inserting the orthogonal projection into (13) gives with (14) and (15) for $\mathbf{v}_h \in V_h$ and $\mathbf{v} \in \mathcal{D}(A) \cap \mathrm{H}^q(\Omega, \mathbb{R}^J)$

$$\begin{aligned}
(A_h\mathbf{v}_h, \mathbf{v})_{0,\Omega} + (A\mathbf{v}, \mathbf{v}_h)_{0,\Omega} &= \sum_K \Big((A_h\mathbf{v}_h, \Pi_{K,h}\mathbf{v})_{0,K} + (A\mathbf{v}, \mathbf{v}_{K,h})_{0,K}\Big) \\
&= \sum_K \Big((\operatorname{div}\mathbf{F}(\mathbf{v}_{K,h}), \Pi_{K,h}\mathbf{v} - \mathbf{v})_{0,K} \\
&\qquad + \sum_{f\in\mathcal{F}_K} (\mathbf{n}_{K,f} \cdot (\mathbf{F}^*_{K,f}(\mathbf{v}_h) - \mathbf{F}(\mathbf{v}_{K,h})), \Pi_{K,h}\mathbf{v} - \mathbf{v})_{0,f}\Big) \\
&= \sum_K \sum_{f\in\mathcal{F}_K} (\mathbf{n}_{K,f} \cdot (\mathbf{F}^*_{K,f}(\mathbf{v}_h) - \mathbf{F}(\mathbf{v}_{K,h})), \Pi_{K,h}\mathbf{v} - \mathbf{v})_{0,f} \\
&\le \sum_K \sum_{f\in\mathcal{F}_K} \|\mathbf{n}_{K,f} \cdot (\mathbf{F}^*_{K,f}(\mathbf{v}_h) - \mathbf{F}(\mathbf{v}_{K,h}))\|_{0,f}\|\Pi_{K,h}\mathbf{v} - \mathbf{v}\|_{0,f} \\
&\le (A_h\mathbf{v}_h, \mathbf{v}_h)_{0,\Omega} + C_{\mathrm{A}}C_{\mathrm{R}}h^{2q-1}\,\|\mathbf{v}\|^2_{q,\Omega}\,.
\end{aligned}$$

Together with $(A\mathbf{v}, \mathbf{v})_{0,\Omega} = 0$ this yields $(A_h\mathbf{v}_h - A\mathbf{v}, \mathbf{v} - \mathbf{v}_h)_{0,\Omega} \le C_{\mathrm{A}}C_{\mathrm{R}}h^{2q-1}\,\|\mathbf{v}\|^2_{q,\Omega}$.
This result is now used for the error estimate. For fixed $T > 0$, we define $\eta_T(t) = T - t$, and the assertion is obtained from

$$\begin{aligned}
\|\mathbf{u} - \mathbf{u}_h\|^2_{\mathrm{L}_2([0,T],V)} &= -\int_0^T \|\mathbf{u}(t) - \mathbf{u}_h(t)\|_V^2 \partial_t\eta_T(t)\,\mathrm{d}t \\
&= \int_0^T \partial_t\|\mathbf{u}(t) - \mathbf{u}_h(t)\|_V^2\,\eta_T(t)\,\mathrm{d}t + T\|\mathbf{u}(0) - \mathbf{u}_h(0)\|_V^2 \\
&= 2\int_0^T \big(M\partial_t\mathbf{u}(t) - M\partial_t\mathbf{u}_h(t), \mathbf{u}(t) - \mathbf{u}_h(t)\big)_{0,\Omega}\eta_T(t)\,\mathrm{d}t + T\|\mathbf{u}(0) - \mathbf{u}_h(0)\|_V^2 \\
&= 2\int_0^T \big(A_h\mathbf{u}_h(t) - A\mathbf{u}(t), \mathbf{u}(t) - \mathbf{u}_h(t)\big)_{0,\Omega}\eta_T(t)\,\mathrm{d}t + T\|\mathbf{u}(0) - \mathbf{u}_h(0)\|_V^2 \\
&\le 2C_{\mathrm{A}}C_{\mathrm{R}}h^{2q-1}\int_0^T \|\mathbf{u}(t)\|^2_{q,\Omega}\eta_T(t)\,\mathrm{d}t + T\|\mathbf{u}(0) - \mathbf{u}_h(0)\|_V^2\,.
\end{aligned}$$

□

4.3 The discrete operators for the wave equations

For the application to acoustic, elastic, and electro-magnetic waves we compute explicit expressions of the local operator $A_{K,h}$ defined in (13) by inserting the solutions of the Riemann problems from the previous section. We verify the assumption (16) in detail for acoustic waves, and we sketch the arguments for electro-magnetic waves. Elastic waves can be analyzed analogously.

Acoustic waves For $(\mathbf{q}_h, p_h) \in V_h$ and $(\boldsymbol{\varphi}_{K,h}, \psi_{K,h}) \in V_{K,h}$ inserting the upwind flux yields

$$\begin{aligned}\big(A_h(\mathbf{q}_h,p_h),(\boldsymbol{\varphi}_{K,h},\psi_{K,h})\big)_{0,K} &= \big(\nabla p_h,\boldsymbol{\varphi}_{K,h}\big)_{0,K} + \big(\operatorname{div}\mathbf{q}_h,\psi_{K,h}\big)_{0,K}\\ &+\sum_{f\in\mathcal{F}_K}\Big(-\frac{c_Kc_{K_f}}{c_K+c_{K_f}}\big([\mathbf{q}_h]_{K,f}\cdot\mathbf{n}_{K,f},\boldsymbol{\varphi}_{K,h}\cdot\mathbf{n}_{K,f}\big)_{0,f}-\frac{1}{c_K+c_{K_f}}\big([p_h]_{K,f},\psi_{K,h}\big)_{0,f}\\ &\quad+\frac{c_K}{c_K+c_{K_f}}\big([p_h]_{K,f},\boldsymbol{\varphi}_{K,h}\cdot\mathbf{n}_{K,f}\big)_{0,f}+\frac{c_{K_f}}{c_K+c_{K_f}}\big([\mathbf{q}_h]_{K,f}\cdot\mathbf{n}_{K,f},\psi_{K,h}\big)_{0,f}\Big).\end{aligned}$$

On Dirichlet boundary faces $f=\partial K\cap\partial\Omega$, we set $[p_h]_{K,f}=2p_{K,h}$ and $[\mathbf{q}_h]_{K,f}\cdot\mathbf{n}_{K,f}=0$. This yields

$$\begin{aligned}\big(A_h(\mathbf{q}_h,p_h),(\mathbf{q}_h,p_h)\big)_{0,\Omega} &= \sum_K\sum_{f\in\mathcal{F}_K}\Big(\big(\mathbf{q}_{K,h}\cdot\mathbf{n}_{K,f},p_{K,h}\big)_{0,f}\\ &\quad-\frac{c_Kc_{K_f}}{c_K+c_{K_f}}\big([\mathbf{q}_h]_{K,f}\cdot\mathbf{n}_{K,f},\mathbf{q}_{K,h}\cdot\mathbf{n}_{K,f}\big)_{0,f}-\frac{1}{c_K+c_{K_f}}\big([p_h]_{K,f},p_{K,h}\big)_{0,f}\\ &\quad+\frac{c_K}{c_K+c_{K_f}}\big([p_h]_{K,f},\mathbf{q}_{K,h}\cdot\mathbf{n}_{K,f}\big)_{0,f}+\frac{c_{K_f}}{c_K+c_{K_f}}\big([\mathbf{q}_h]_{K,f}\cdot\mathbf{n}_{K,f},p_{K,h}\big)_{0,f}\Big)\\ &= \frac{1}{2}\sum_K\sum_{f\in\mathcal{F}_K}\Big(\frac{c_Kc_{K_f}}{c_K+c_{K_f}}\big\|[\mathbf{q}_h]_{K,f}\cdot\mathbf{n}_{K,f}\big\|_{0,f}^2+\frac{1}{c_K+c_{K_f}}\big\|[p_h]_{K,f}\big\|_{0,f}^2\Big).\end{aligned}\tag{17}$$

Here, we used $[\mathbf{q}_h]_{K,f}=-[\mathbf{q}_h]_{K_f,f}$, $[p_h]_{K,f}=-[p_h]_{K_f,f}$, $\mathbf{n}_{K,f}=-\mathbf{n}_{K_f,f}$,

$$\begin{aligned}\big([\mathbf{q}_h]_{K,f}\cdot\mathbf{n}_{K,f},\mathbf{q}_{K,h}\cdot\mathbf{n}_{K,f}\big)_{0,f}+\big([\mathbf{q}_h]_{K_f,f}\cdot\mathbf{n}_{K_f,f},\mathbf{q}_{K_f,h}\cdot\mathbf{n}_{K_f,f}\big)_{0,f} &= -\|[\mathbf{q}_h]_{K_f,f}\cdot\mathbf{n}_{K_f,f}\|_{0,f}^2\,,\\ \big([p_h]_{K,f},p_{K,h}\big)_{0,f}+\big([p_h]_{K_f,f},p_{K_f,h}\big)_{0,f} &= -\|[p_h]_{K,f}\|_{0,f}^2\,,\end{aligned}$$

and

$$\begin{aligned}&\sum_K\sum_{f\in\mathcal{F}_K}\Big(\big(\mathbf{q}_{K,h}\cdot\mathbf{n}_{K,f},p_{K,h}\big)_{0,f}+\frac{c_K}{c_K+c_{K_f}}\big([p_h]_{K,f},\mathbf{q}_{K,h}\cdot\mathbf{n}_{K,f}\big)_{0,f}+\frac{c_{K_f}}{c_K+c_{K_f}}\big([\mathbf{q}_h]_{K,f}\cdot\mathbf{n}_{K,f},p_{K,h}\big)_{0,f}\Big)\\ &\quad=\sum_K\sum_{f\in\mathcal{F}_K}\Big(\frac{c_K}{c_K+c_{K_f}}\big(p_{K,h}+[p_h]_{K,f},\mathbf{q}_{K,h}\cdot\mathbf{n}_{K,f}\big)_{0,f}+\frac{c_{K_f}}{c_K+c_{K_f}}\big((\mathbf{q}_{K,h}+[\mathbf{q}_h]_{K,f})\cdot\mathbf{n}_{K,f},p_{K,h}\big)_{0,f}\Big)\\ &\quad=\sum_K\sum_{f\in\mathcal{F}_K}\Big(\frac{c_K}{c_K+c_{K_f}}\big(p_{K_f,h},\mathbf{q}_{K,h}\cdot\mathbf{n}_{K,f}\big)_{0,f}+\frac{c_{K_f}}{c_K+c_{K_f}}\big(\mathbf{q}_{K_f,h}\cdot\mathbf{n}_{K,f},p_{K,h}\big)_{0,f}\Big)=0\,.\end{aligned}$$

We have for the norm of the flux

$$\big\|\mathbf{n}_{K,f}\cdot\big(\mathbf{F}^*_{K,f}(\mathbf{q}_h,p_h)-\mathbf{F}(\mathbf{q}_{K,h},p_{K,h})\big)\big\|_{0,f}^2\le C(c_K,c_{K_f})\Big(\big\|[\mathbf{q}_h]_{K,f}\cdot\mathbf{n}_{K,f}\|_{0,f}^2+\big\|[p_h]_{K,f}\big\|_{0,f}^2\Big)$$

Together with (17) this allows to verify assumption (16).

Elastic waves For $(\boldsymbol{\sigma}_h, \mathbf{v}_h) \in V_h$ and $(\boldsymbol{\varphi}_{K,h}, \boldsymbol{\psi}_{K,h}) \in V_{K,h}$ the discrete operator with upwind flux is defined by

$$
\begin{aligned}
\big(A_h(\boldsymbol{\sigma}_h, \mathbf{v}_h), (\boldsymbol{\varphi}_{K,h}, \boldsymbol{\psi}_{K,h})\big)_{0,K} &= -\big(\boldsymbol{\varepsilon}(\mathbf{v}_{K,h}), \boldsymbol{\varphi}_{K,h}\big)_{0,K} - \big(\operatorname{div} \boldsymbol{\sigma}_{K,h}, \boldsymbol{\psi}_{K,h}\big)_{0,K} \\
&- \sum_{f \in \mathcal{F}_K} \Big(\frac{(2\mu_{K_f} + \lambda_{K_f}) c_{\mathrm{P},K}}{c_{\mathrm{P},K}(2\mu_{K_f} + \lambda_{K_f}) + (2\mu_K + \lambda_K) c_{\mathrm{P},K_f}} \big(\mathbf{n}_{K,f} \cdot [\mathbf{v}_h]_{K,f}, \mathbf{n}_{K,f} \cdot (\boldsymbol{\varphi}_{K,h} \mathbf{n}_{K,f})\big)_{0,f} \\
&+ \frac{(2\mu_{K_f} + \lambda_{K_f})(2\mu_K + \lambda_K)}{c_{\mathrm{P},K}(2\mu_{K_f} + \lambda_{K_f}) + (2\mu_K + \lambda_K) c_{\mathrm{P},K_f}} \big(\mathbf{n}_{K,f} \cdot [\mathbf{v}_h]_{K,f}, \mathbf{n}_{K,f} \cdot \boldsymbol{\psi}_{K,h}\big)_{0,f} \\
&+ \frac{\mu_{K_f} c_{\mathrm{S},K}}{c_{\mathrm{S},K} \mu_{K_f} + \mu_K c_{\mathrm{S},K_f}} \big([\mathbf{v}_h]_{K,f} - (\mathbf{n}_{K,f} \cdot [\mathbf{v}_h]_{K,f}) \mathbf{n}_{K,f}, \boldsymbol{\varphi}_{K,h} \mathbf{n}_{K,f} - (\mathbf{n}_{K,f} \cdot (\boldsymbol{\varphi}_{K,h} \mathbf{n}_{K,f})) \mathbf{n}_{K,f}\big)_{0,f} \\
&+ \frac{\mu_{K_f} \mu_K}{c_{\mathrm{S},K} \mu_{K_f} + \mu_K c_{\mathrm{S},K_f}} \big([\mathbf{v}_h]_{K,f} - (\mathbf{n}_{K,f} \cdot [\mathbf{v}_h]_{K,f}) \mathbf{n}_{K,f}, \boldsymbol{\psi}_{K,h} - (\mathbf{n}_{K,f} \cdot \boldsymbol{\psi}_{K,h}) \mathbf{n}_{K,f}\big)_{0,f} \\
&+ \frac{c_{\mathrm{P},K_f} c_{\mathrm{P},K}}{c_{\mathrm{P},K}(2\mu_{K_f} + \lambda_{K_f}) + (2\mu_K + \lambda_K) c_{\mathrm{P},K_f}} \big(\mathbf{n}_{K,f} \cdot ([\boldsymbol{\sigma}_h]_{K,f} \mathbf{n}_{K,f}), \mathbf{n}_{K,f} \cdot (\boldsymbol{\varphi}_{K,h} \mathbf{n}_{K,f})\big)_{0,f} \\
&+ \frac{c_{\mathrm{P},K_f}(2\mu_K + \lambda_K)}{c_{\mathrm{P},K}(2\mu_{K_f} + \lambda_{K_f}) + (2\mu_K + \lambda_K) c_{\mathrm{P},K_f}} \big(\mathbf{n}_{K,f} \cdot ([\boldsymbol{\sigma}_h]_{K,f} \mathbf{n}_{K,f}), \mathbf{n}_{K,f} \cdot \boldsymbol{\psi}_{K,h}\big)_{0,f} \\
&+ \frac{c_{\mathrm{S},K_f} c_{\mathrm{S},K}}{c_{\mathrm{S},K} \mu_{K_f} + \mu_K c_{\mathrm{S},K_f}} \big([\boldsymbol{\sigma}_h]_{K,f} \mathbf{n}_{K,f} - (\mathbf{n}_{K,f} \cdot ([\boldsymbol{\sigma}_h]_{K,f} \mathbf{n}_{K,f})) \mathbf{n}_{K,f}, \boldsymbol{\varphi}_{K,h} \mathbf{n}_{K,f} - (\mathbf{n}_{K,f} \cdot (\boldsymbol{\varphi}_{K,h} \mathbf{n}_{K,f})) \mathbf{n}_{K,f}\big)_{0,f} \\
&+ \frac{c_{\mathrm{S},K_f} \mu_K}{c_{\mathrm{S},K} \mu_{K_f} + \mu_K c_{\mathrm{S},K_f}} \big([\boldsymbol{\sigma}_h]_{K,f} \mathbf{n}_{K,f} - (\mathbf{n}_{K,f} \cdot ([\boldsymbol{\sigma}_h]_{K,f} \mathbf{n}_{K,f})) \mathbf{n}_{K,f}, \boldsymbol{\psi}_{K,h} - (\mathbf{n}_{K,f} \cdot \boldsymbol{\psi}_{K,h}) \mathbf{n}_{K,f}\big)_{0,f} \Big) .
\end{aligned}
$$

On Dirichlet boundary faces $f = \partial K \cap \partial \Omega_{\mathrm{D}}$, we set $[\mathbf{v}_h]_{K,f} = 2\mathbf{v}_{K,h}$ and $[\boldsymbol{\sigma}_h]_{K,f} \cdot \mathbf{n}_{K,f} = \mathbf{0}$, and on Neumann boundary faces $f = \partial K \cap \partial \Omega_{\mathrm{N}}$, we set $[\mathbf{v}_h]_{K,f} = \mathbf{0}$ and $[\boldsymbol{\sigma}_h]_{K,f} \cdot \mathbf{n}_{K,f} = 2\boldsymbol{\sigma}_{K,h} \cdot \mathbf{n}_{K,f}$. Note that the solution of Riemann problem for elastic waves in 3D also yields this full upwind operator [34].

Electro-magnetic waves For $(\mathbf{H}_h, \mathbf{E}_h) \in V_h$ and $(\boldsymbol{\varphi}_{K,h}, \boldsymbol{\psi}_{K,h}) \in V_{K,h}$ we have

$$
\begin{aligned}
\big(A_h(\mathbf{H}_h, \mathbf{E}_h), (\boldsymbol{\varphi}_{K,h}, \boldsymbol{\psi}_{K,h})\big)_{0,K} &= (\operatorname{curl} \mathbf{E}_{K,h}, \boldsymbol{\varphi}_{K,h})_{0,K} - \big(\operatorname{curl} \mathbf{H}_{K,h}, \boldsymbol{\psi}_{K,h}\big)_{0,K} \\
&+ \sum_{f \in \mathcal{F}_K} \Big(\frac{c_{K_f} \varepsilon_{K_f}}{c_K \varepsilon_K + c_{K_f} \varepsilon_{K_f}} \big(\mathbf{n}_{K,f} \times [\mathbf{E}_h]_{K,f}, \boldsymbol{\varphi}_{K,h}\big)_{0,f} - \frac{c_{K_f} \mu_{K_f}}{c_K \mu_K + c_{K_f} \mu_{K_f}} \big(\mathbf{n}_{K,f} \times [\mathbf{H}_h]_{K,f}, \boldsymbol{\psi}_{K,h}\big)_{0,f} \\
&+ \frac{1}{c_K \mu_K + c_{K_f} \mu_{K_f}} \big(\mathbf{n}_{K,f} \times (\mathbf{n}_{K,f} \times [\mathbf{E}_h]_{K,f}), \boldsymbol{\psi}_{K,h}\big)_{0,f} \\
&+ \frac{1}{c_K \varepsilon_K + c_{K_f} \varepsilon_{K_f}} \big(\mathbf{n}_{K,f} \times (\mathbf{n}_{K,f} \times [\mathbf{H}_h]_{K,f}), \boldsymbol{\varphi}_{K,h}\big)_{0,f} \Big) .
\end{aligned}
$$

The perfect conducting boundary conditions on the faces $f = \partial K \cap \partial \Omega$ are modeled by the (only virtual) definition of $\mathbf{n}_{K,f} \times \mathbf{E}_{K_f} = -\mathbf{n}_{K,f} \times \mathbf{E}_K$ and $\mathbf{n}_{K,f} \times \mathbf{H}_{K_f} = \mathbf{n}_f \times \mathbf{H}_K$, i.e., $\mathbf{n}_{K,f} \times [\mathbf{E}]_{K,f} = -2\mathbf{n}_{K,f} \times \mathbf{E}_K$ and $\mathbf{n}_{K,f} \times [\mathbf{H}]_{K,f} = \mathbf{0}$. With the same arguments as for the acoustic case we obtain

$$
\big(A_h(\mathbf{H}_h, \mathbf{E}_h), (\mathbf{H}_h, \mathbf{E}_h)\big)_{0,\Omega} = \frac{1}{2} \sum_K \sum_{f \in \mathcal{F}_K} \left(\frac{\big\|\mathbf{n}_{K,f} \times [\mathbf{E}_h]_{K,f}\big\|_{0,f}^2}{c_K \mu_K + c_{K_f} \mu_{K_f}} + \frac{\big\|\mathbf{n}_{K,f} \times [\mathbf{H}_h]_{K,f}\big\|_{0,f}^2}{c_K \varepsilon_K + c_{K_f} \varepsilon_{K_f}} \right)
$$

using $\big(\mathbf{n}_{K,f} \times (\mathbf{n}_{K,f} \times [\boldsymbol{\psi}_h]_{K,f}), \boldsymbol{\psi}_{K,h}\big)_{0,f} + \big(\mathbf{n}_{K_f,f} \times (\mathbf{n}_{K_f,f} \times [\boldsymbol{\psi}_h]_{K_f,f}), \boldsymbol{\psi}_{K_f,h}\big)_{0,f} = \big\|\mathbf{n}_{K,f} \times [\boldsymbol{\psi}_h]_{K,f}\big\|_{0,f}^2$ and

$$
\begin{aligned}
\sum_K \sum_{f \in \mathcal{F}_K} \Big(&\big(\mathbf{n}_{K,f} \times \mathbf{E}_{K,h}, \mathbf{H}_{K,h}\big)_{0,f} \\
&+ \frac{c_{K_f} \varepsilon_{K_f}}{c_K \varepsilon_K + c_{K_f} \varepsilon_{K_f}} \big(\mathbf{n}_{K,f} \times [\mathbf{E}_h]_{K,f}, \mathbf{H}_{K,h}\big)_{0,f} - \frac{c_{K_f} \mu_{K_f}}{c_K \mu_K + c_{K_f} \mu_{K_f}} \big(\mathbf{n}_{K,f} \times [\mathbf{H}_h]_{K,f}, \mathbf{E}_{K,h}\big)_{0,f} \Big) = 0 .
\end{aligned}
$$

Again, this gives (16) with C_{A} depending only on the material parameters.

5 Time integration for linear systems

In this section we summarize efficient time integration methods for the discrete evolution equation (12). Let $\phi_1, \dots, \phi_N$ be a discontinuous finite element basis of V_h. With

$$\mathbb{M} = \Big((M\phi_k, \phi_j)_{0,\Omega}\Big)_{j,k}, \qquad \mathbb{A} = \Big((A_h\phi_k, \phi_j)_{0,\Omega}\Big)_{j,k}$$

denoting the (symmetric, positive definite, block-diagonal) mass matrix, and the non-symmetric stiffness matrix, respectively, we can write (12) as

$$\mathbb{M}\partial_t u + \mathbb{A}u = 0, \quad u(0) = u_0, \tag{18}$$

where

$$u(t) = \big(u_j(t)\big)_{j=1}^N, \qquad \mathbf{u}_h(t) = \sum_{j=1}^N u_j(t)\phi_j \in V_h$$

denote the coefficient vector of the solution at time t with respect to the finite element basis and its corresponding discontinuous finite element function $\mathbf{u}_h$. The corresponding inner product is defined by $(u, v)_{\mathbb{M}} := v^T\mathbb{M}u$, so that $\|\mathbf{u}_h(t)\|_V = \|u(t)\|_{\mathbb{M}}$.

The solution of this finite dimensional linear problem is given by

$$u(t) = \exp(-t\mathbb{M}^{-1}\mathbb{A})u_0, \quad t \geq 0, \tag{19}$$

where $\exp(\cdot)$ is the familiar matrix exponential function. For a fixed time step $\tau > 0$ we seek approximations

$$u^n \approx u(t_n), \qquad t_n = n\tau, \quad n = 0, 1, \dots.$$

For simplicity, we restrict ourselves to onestep methods. Then the approximations to the solution of (18) can be written as

$$u^{n+1} = \Phi_n(-\tau\mathbb{M}^{-1}\mathbb{A})u^n, \quad n = 0, 1, \dots, \tag{20}$$

where Φ_n denotes the stability function of the method.

Explicit Runge-Kutta methods For an m-stage explicit Runge-Kutta method, Φ_n is a *fixed* polynomial of *fixed* degree m, which approximates the exponential function in a neighborhood of zero. For instance, for the classical forth-order Runge-Kutta method we have $m = 4$ and

$$\Phi_n(\xi) = 1 + \xi + \frac{1}{2}\xi^2 + \frac{1}{6}\xi^3 + \frac{1}{24}\xi^4, \qquad \text{for all } n.$$

Each time step requires m multiplications with $\mathbb{A}$ and m solutions of linear systems with the block-diagonal matrix $\mathbb{M}$. These methods are simple to implement and computationally cheap but the main disadvantage is the stability issue: all explicit Runge-Kutta schemes have a bounded stability region requiring time steps proportional to h^{-1} for first-order systems (CFL condition).

Implicit Runge-Kutta methods Implicit m-stage Runge-Kutta methods use a *fixed* rational function Φ_n with *fixed* numerator and denominator degree at most m to approximate the exponential function. For hyperbolic problems as considered in this paper, Gauß collocation methods are particularly attractive [17, Chap. IV]. Here, Φ_n is the (m, m) Padé approximation to the exponential function. It is well-known that Gauß methods are A-stable and thus do not suffer from restrictions on the time step size τ for stability reasons. The price to pay is that implicit methods are more expensive and thus the efficient solution of the linear systems arising is crucial. We consider two specific examples, namely the implicit midpoint rule

$$u^{n+1} = u^n - \tau\big(\mathbb{M} + \tfrac{\tau}{2}\mathbb{A}\big)^{-1}\mathbb{A}\,u^n\,,$$

and the 3-stage Gauss method where

$$u^{n+1} = u^n - \tau\Big(\mathbb{M} + \tfrac{\tau}{\alpha_1}\mathbb{A}\Big)^{-1}\Big(\mathbb{M} + \tfrac{\tau}{\alpha_0}\mathbb{A}\Big)\Big(\mathbb{M} + \tfrac{\tau}{\alpha_2}\mathbb{A}\Big)^{-1}\Big(\mathbb{M} - \tfrac{\tau}{\alpha_0}\mathbb{A}\Big)\Big(\mathbb{M} + \tfrac{\tau}{\alpha_3}\mathbb{A}\Big)^{-1}\mathbb{A}u^n\,,$$

with $\alpha_0 = \mathrm{i}\sqrt{60}$, and

$$\alpha_1 = 4 - 2\sqrt[3]{\frac{2}{1+\sqrt{5}}} + 2^{2/3}\sqrt[3]{1+\sqrt{5}} \approx 4.6444$$

$$\alpha_2 = 4 + (1-\mathrm{i}\sqrt{3})\sqrt[3]{\frac{2}{1+\sqrt{5}}} - (1+\mathrm{i}\sqrt{3})\sqrt[3]{\frac{1}{2}(1+\sqrt{5})} \approx 3.6778 - 3.5088\mathrm{i}, \quad \alpha_3 = \bar{\alpha}_2\,.$$

Each time step requires one matrix-vector multiplication with A, two with $\mathbb{M} + \gamma\tau\mathbb{A}$ for some (complex) coefficient γ and three solutions of linear systems with such coefficient matrices. Note that the stability property (16) for the upwind discretization shows that the linear system is dissipative, so that the implicit Gauss collocation methods are well-defined for all time steps $\tau > 0$.

Polynomial Krylov methods An alternative to explicit or implicit Runge-Kutta methods, for which the stability function Φ_n in (20) is fixed for all time steps, is to choose Φ_n adaptively. This can be accomplished by Krylov subspace methods.

Standard Krylov subspace methods compute an approximation to $x = \exp(-\tau\mathbb{M}^{-1}\mathbb{A})u^n$ in the polynomial Krylov space

$$\mathcal{K}_m := \mathcal{K}_m(\mathbb{M}^{-1}\mathbb{A}, u^n) = \mathrm{span}\{u^n, \mathbb{M}^{-1}\mathbb{A}u^n, \ldots, (\mathbb{M}^{-1}\mathbb{A})^{m-1}u^n\}.$$

The approximation proceeds in two steps. First, a basis of $\mathcal{K}_m$ is computed by the Lanczos or by the Arnoldi algorithm. Here, we only consider the Arnoldi algorithm with respect to the inner product $(\cdot,\cdot)_{\mathbb{M}}$. This yields a matrix $V_m = [v_1, \ldots, v_m] \in \mathbb{R}^{N\times m}$ and an upper Hessenberg matrix $H_m \in \mathbb{R}^{m\times m}$ such that

$$\mathbb{A}V_m = \mathbb{M}V_m H_m + h_{m+1,m}\mathbb{M}v_{m+1}e_m^T, \quad V_m^T\mathbb{M}V_m = I_m. \tag{21}$$

The $\mathbb{M}$-orthogonality of V_m shows that $H_m = V_m^T\mathbb{A}V_m$. Now the approximation is given as

$$\exp(-\tau\mathbb{M}^{-1}\mathbb{A})u^n \approx V_m \exp(-\tau H_m)V_m^T\mathbb{M}u^n\,,$$

see [11,32]. Inserting $V_m^T\mathbb{M}u^n = \|u^n\|_{\mathbb{M}}\, e_1$ this yields the polynomial Krylov approximation

$$u^{n+1} = \|u^n\|_{\mathbb{M}}\, V_m \exp(-\tau H_m)e_1 = \Phi_n(-\tau\mathbb{M}^{-1}\mathbb{A})u^n \tag{22}$$

for some polynomial Φ_n of degree at most $m-1$, which is chosen automatically. Since $m \ll N$, for the small matrix exponential $\exp(-\tau H_m)$ established approximation techniques can be applied (e.g., rational Chebyshev approximation, Padé approximation or diagonalization [20]).

The cost of m-steps of the Arnoldi algorithm is the same as for an m-stage explicit Runge-Kutta method in terms of matrix vector multiplications and solutions of linear systems with $\mathbb{M}$. In addition, we have to compute inner products and linear combinations of vectors. In [21] it was shown that the error of Krylov approximations to the matrix exponential always decays superlinearly and that the superlinear error decay starts at $m \approx \left\|\tau\mathbb{M}^{-1}\mathbb{A}\right\|$ iteration steps for discretizations of hyperbolic problems. Hence, the time step τ is not restricted by stability but by the maximum number of Arnoldi steps. Another significant advantage is that Krylov approximations exploit properties of the starting vector, while the fixed polynomials of Runge-Kutta methods do not. For instance, if the starting vector corresponds to a smooth function, then the convergence is significantly better than for an arbitrary starting vector [12]. Moreover, it is well-known that Krylov approximations are quasioptimal, i.e., for a fixed degree m, they provide the optimal polynomial approximation to u^{n+1} up to a constant.

An implementation of the Arnoldi algorithm with respect to the $\mathbb{M}$ inner product to compute (22) is given in Alg. 1. To avoid pathological cases, the algorithm may be extended by checking if $h_{m+1,m}$ is not too small. The algorithm might also be combined with substepping, i.e., dividing a time step of length τ into $M > 1$ smaller time steps of length τ/M, as proposed and implemented in [1, 35].

The stopping criteria in Line 17 of Alg. 1, was introduced in [37], see also [2] for a detailed investigation of residuals of the matrix exponential. Here, δ_m is an estimation of the relative error $\|x_m - x\|_{\mathbb{M}} / \|x_0 - x\|_{\mathbb{M}}$ in the mth Krylov step. Note that y_m has to be measured in the Euclidean norm; since for $x_m = V_m y_m$, we have $\|x_m\|_{\mathbb{M}} = \|y_m\|$.

Algorithm 1 Polynomial Krylov method

Input: $\mathbb{M}$, $\mathbb{A}$, v, τ, MaxIter, Tol
Output: $x_m \approx \exp(-\tau\mathbb{M}^{-1}\mathbb{A})v$, $m \leq$ MaxIter, estimated error $\leq$ Tol
$\beta = \|v\|_{\mathbb{M}}, \quad v_1 = v/\beta$
for $m = 1, 2, \ldots,$ MaxIter **do**
  $w = \mathbb{A}v_m$
  solve $\mathbb{M}v_{m+1} = w$
  for $k = 1, \ldots, m$ **do**
    $h_{k,m} = v_k^T w$
    $v_{m+1} = v_{m+1} - h_{k,m}v_k$
  end for
  $h_{m+1,m} = \|v_{m+1}\|_{\mathbb{M}}$
  $v_{m+1} = v_{m+1}/h_{m+1,m}$
  $y_m = \beta \exp(-\tau H_m)e_1$
  $\delta_m = \|y_m - [y_{m-1}; 0]\| \,/\, \|y_m\|$
  $\epsilon_m = 1 + \|y_m\|$
  if $\delta_m < 1$ **then**
    $\epsilon_m = \min\left(1 + \|y_m\|, \delta_m/(1-\delta_m)\,\|y_m\|\right)$
  end if
  if $\epsilon_m \leq$ Tol **then**
    break
  end if
end for
if $m \geq$ MaxIter and $\epsilon_m >$ Tol **then**
  no convergence
end if
$x_m = [v_1, \ldots, v_m]y_m$

Rational Krylov methods A drawback of polynomial Krylov methods is that the number of iteration steps to reach the superlinear convergence behavior is proportional to $\left\|\tau\mathbb{M}^{-1}\mathbb{A}\right\|$ for our applications. If the maximum number of iterations is not sufficient to reach this regime, one either has to reduce the time step τ (i.e., add a substepping algorithm like in [1, 35]) or use some kind of restarting procedure, see, e.g., [8].

Due to these shortcomings, rational Krylov methods became popular recently, cf. [16] for a review. For a fixed shift parameter $\gamma > 0$, we approximate the exponential flow $\exp(-\tau\mathbb{M}^{-1}\mathbb{A})u^n$ in the rational Krylov space

$$\mathcal{K}_m((\gamma I + \tau\mathbb{M}^{-1}\mathbb{A})^{-1}, u^n).$$

The Arnoldi algorithm yields an $\mathbb{M}$-orthonormal basis V_m and an upper Hessenberg matrix H_m such that

$$(\gamma\mathbb{M} + \tau\mathbb{A})^{-1}\mathbb{M}V_m = V_m H_m + h_{m+1,m}v_{m+1}e_m^T, \quad V_m^T\mathbb{M}V_m = I_m. \tag{23}$$

The projection matrix $\widehat{H}_m := V_m^T\mathbb{A}V_m$ can be extracted from the quantities of the Arnoldi method via

$$-\tau\widehat{H}_m = \gamma I_m - H_m^{-1} + \tau V_m^T\mathbb{A}v_{m+1}e_m^T H_m^{-1} \tag{24}$$

leading to the rational Krylov approximation

$$\exp(-\tau\mathbb{M}^{-1}\mathbb{A})u^n \approx u^{n+1} = V_m \exp(-\tau\widehat{H}_m)V_m^T\mathbb{M}u^n = \|u^n\|_{\mathbb{M}}\, V_m \exp(-\tau\widehat{H}_m)e_1.$$

For the exponential function, it can be shown that under certain regularity assumptions, the convergence is independent of the spatial mesh [14].

The additional matrix vector multiplication with $\mathbb{A}$ in (24) can be avoided by neglecting the last term:

$$-\tau\widehat{H}_m \approx \gamma I_m - H_m^{-1}. \tag{25}$$

In practice, we did not see a significant difference in the convergence behavior if we use this approximation instead of the projection matrix $\widehat{H}_m$.

Algorithm 2 Rational Krylov method for computing $x_m \approx \exp(-\tau \mathbb{M}^{-1}\mathbb{A})v$

1: **Input:** $\mathbb{M}$, $\mathbb{A}$, v, τ, MaxIter, Tol, θ
2: **Output:** $x_m \approx \exp(-\tau \mathbb{M}^{-1}\mathbb{A})v$, $m \leq$ MaxIter, estimated error $\leq$ Tol
3: $w = \mathbb{M}v, \quad \beta = \sqrt{v^T w}, \quad v_1 = v/\beta, \quad w = w/\beta, \quad \epsilon_0 = 1 - \text{Tol}$
4: **for** $m = 1, 2, \ldots,$ MaxIter **do**
5: solve $(\gamma\mathbb{M} + \tau\mathbb{A})v_{m+1} = w$ for v_{m+1} approximately s. t. $\|(\gamma\mathbb{M} + \tau\mathbb{A})v_{m+1} - w\| \leq \theta\text{Tol}/(\epsilon_{m-1} + \text{Tol})$
6: $w = \mathbb{M}v_{m+1}$
7: **for** $k = 1, \ldots, m$ **do**
8: $h_{k,m} = v_k^T w$
9: $v_{m+1} = v_{m+1} - h_{k,m} v_k$
10: **end for**
11: $w = \mathbb{M}v_{m+1}$
12: $h_{m+1,m} = \sqrt{v_{m+1}^T w}$
13: $v_{m+1} = v_{m+1}/h_{m+1,m}, \quad w = w/h_{m+1,m}$
14: compute $-\tau\widehat{H}_m$ from (24) or approximate it by (25)
15: $y_m = \beta \exp(-\tau\widehat{H}_m)e_1$
16: $\delta_m = \|y_m - [y_{m-1}; 0]\| \,/\, \|y_m\|$
17: $\epsilon_m = 1 + \|y_m\|$
18: **if** $\delta_m < 1$ **then**
19: $\epsilon_m = \min\left(1 + \|y_m\|, \delta_m/(1-\delta_m)\,\|y_m\|\right)$
20: **end if**
21: **if** $\epsilon_m \leq$ Tol **then**
22: break
23: **end if**
24: **end for**
25: **if** $m \geq$ MaxIter and $\epsilon_m >$ Tol **then**
26: no convergence
27: **end if**
28: $x_m = [v_1, \ldots, v_m]y_m$

The full algorithm is given in Alg. 2. The stopping criteria for the outer iteration (the rational Krylov method) is the same as for the polynomial Krylov method above, see [2, 37]. If the linear systems arising in each step of the rational Krylov method are solved by an inner iteration, e.g., by a preconditioned iterative solver, then the efficiency can be improved by using a relaxed stopping criterion proposed in [37]. This is implemented in Line 5 of Alg. 2 (with a safty factor $\theta \in (0, 1]$). More details on the preconditioner are given in the following section.

The choice of the shift γ and the step size τ is a nontrivial task and subject of current research, see [12, Section 5] for a theoretical investigation.

6 Numerical experiments

All our simulations have been implemented using the parallel finite element software M++ [40]. For the implicit time integration methods the linear systems with coefficient matrix $\gamma\mathbb{M} + \tau\mathbb{A}$ are solved with a Krylov method and multigrid preconditioner [39] with block Jacobi smoothing. We use a p-version of the multigrid method with a finite volume hierarchy (using a direct parallel solver for the coarse problem [29]) and the transfer to the DG space on the finest level [28]. Since the discontinuous Galerkin spaces are nested, the embedding directly yields the multigrid prolongation. On the other hand, the discretization is nonconforming and $\mathbb{A}$ is non-symmetric, so that standard multigrid theory does not apply. Nevertheless, if τ/γ is sufficiently small and the coarse problem is sufficiently fine, we always obtain convergence, but we clearly observe that the spectral bounds for the multigrid preconditioner applied to the matrix $\gamma\mathbb{M} + \tau\mathbb{A}$ depend on γ and τ.

6.1 Maxwell equation in 2D

In the first experiment, we investigate the convergence in time and space for a 2D reduction of Maxwell's equations, where we assume that the fields are constant in z-direction. Then, we set $\mathbf{u} = (\mathbf{H}_x, \mathbf{H}_y, \mathbf{E}_z)$ and $\mathbf{H}_z \equiv \mathbf{E}_x \equiv \mathbf{E}_y \equiv 0$. We use the parameters $\mu = \varepsilon = 1$, an unstructured triangular mesh in a locally tapered domain $\Omega \subset (0, 10) \times (-1, 1)$ with

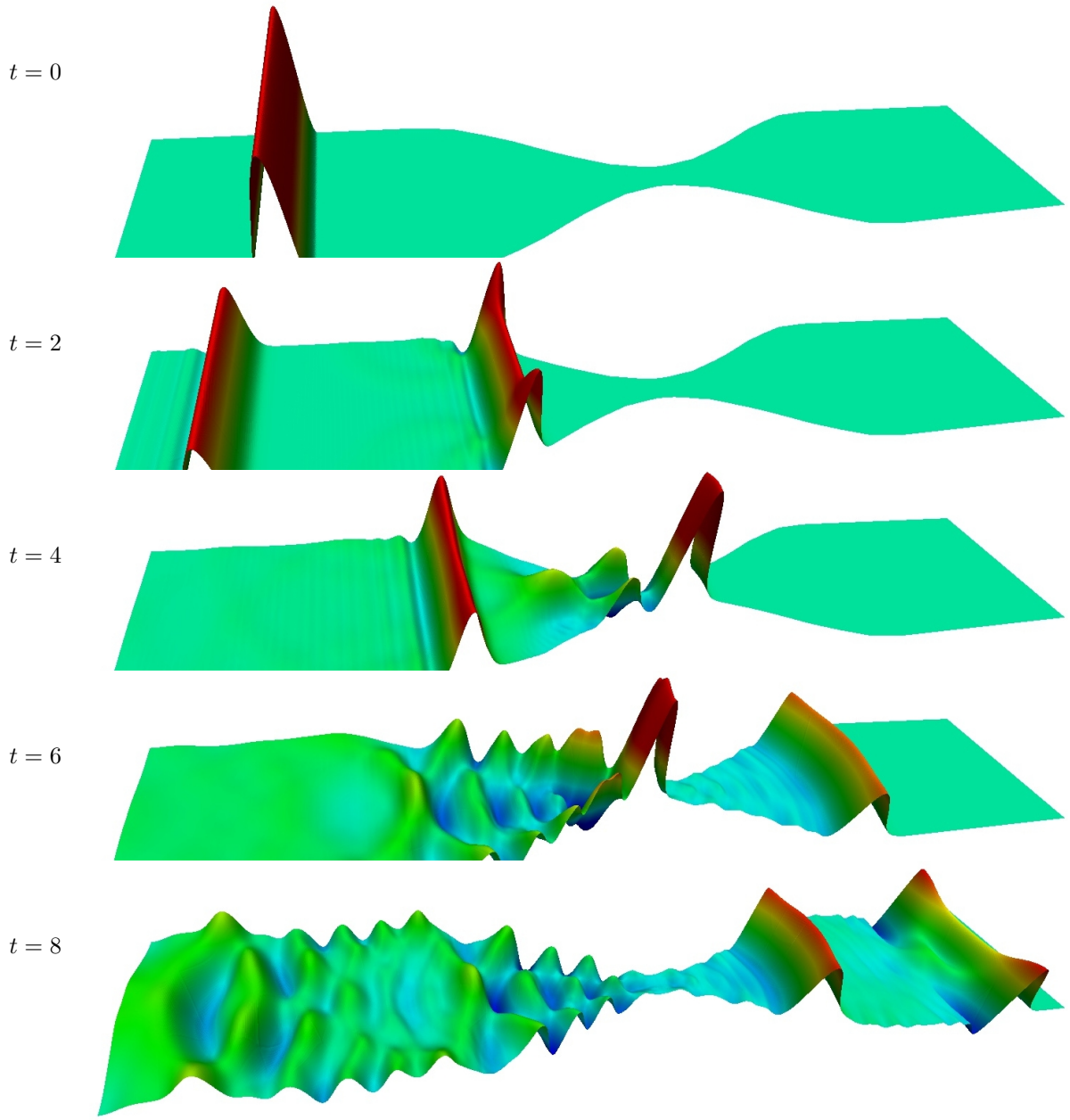

Fig. 1 Initial distribution of $\mathbf{E}_z$ and time evolution at selected time steps.

quadratic polynomial approximations in each cell, and perfectly magnetic boundary conditions ($\mathbf{H} \times \mathbf{n} = \mathbf{0}$). We start with a local pulse

$$\mathbf{u}_0(x,y,z) = \begin{pmatrix} 0 \\ 0 \\ \cos(\pi(4x-3))+1 \end{pmatrix} \quad \text{for } 0.5 < x < 1\,, \qquad \mathbf{u}_0(x,y,z) = \mathbf{0} \quad \text{else.}$$

Results at sample times are shown in Fig. 1.

Let V_0 be the finite element space of the coarse mesh, and by uniform refinement we obtain the finite element spaces $V_1, V_2, \ldots, V_L$ of dimension N_l. In time, we use K_j uniform time steps $\tau_j = T/K_j$, $j = 0, \ldots, J$. The solution on level l in V_l at the final time $T = 8$ computed with K_j time steps is denoted by $\mathbf{u}_{j,l}$. In all tests we use $J = 4$ and $L = 3$ with $N_0 = 27\,216$, $N_1 = 108\,864$, $N_2 = 435\,456$, and $N_3 = 1\,741\,824$.

		$K_0 = 3\,200$	$K_1 = 6\,400$	$K_2 = 12\,800$	$K_3 = 25\,600$	$K_4 = 51\,200$
$m = 2$	multiplications with $\mathbb{M}^{-1}\mathbb{A}$	6 400	12 800	25 600	51 200	102 400
	$\|\mathbf{u}_{j,0}\|_V$	1.16307	1.16302	1.16302	1.16302	1.16302
	$\|\mathbf{u}_{j,1}\|_V$	unstable	1.21983	1.21981	1.21981	1.21981
	$\|\mathbf{u}_{j,2}\|_V$	unstable	unstable	1.22450	1.22450	1.22450
	$\|\mathbf{u}_{j,3}\|_V$	unstable	unstable	unstable	1.22473	1.22473
	$\|\mathbf{u}_{j+1,0} - \mathbf{u}_{j,0}\|_V$		5.18e-03	1.30e-03	3.24e-04	8.09e-05
	$\|\mathbf{u}_{j+1,1} - \mathbf{u}_{j,1}\|_V$			2.29e-03	5.72e-04	1.43e-04
	$\|\mathbf{u}_{j+1,2} - \mathbf{u}_{j,2}\|_V$				6.82e-04	1.71e-04
	$\|\mathbf{u}_{j+1,3} - \mathbf{u}_{j,3}\|_V$					2.00e-04
	$f_{j,0}$			4.0006	4.0001	4.0001
	$f_{j,1}$				4.0003	4.0001
	$f_{j,2}$					4.0002
	$\|\mathbf{u}_{j,1} - \mathbf{u}_{j,0}\|_V$		1.81e-01	1.81e-01	1.81e-01	1.80e-01
	$\|\mathbf{u}_{j,2} - \mathbf{u}_{j,1}\|_V$			2.46e-02	2.46e-02	2.46e-02
	$\|\mathbf{u}_{j,3} - \mathbf{u}_{j,2}\|_V$				4.66e-03	4.66e-03
$m = 4$	multiplications with $\mathbb{M}^{-1}\mathbb{A}$	12 800	25 600	51 200	102 400	204 800
	$\|\mathbf{u}_{j,0}\|_V$	1.16302	1.16302	1.16302	1.16302	1.16302
	$\|\mathbf{u}_{j,1}\|_V$	unstable	1.21981	1.21981	1.21981	1.21981
	$\|\mathbf{u}_{j,2}\|_V$	unstable	unstable	1.22450	1.22450	1.22450
	$\|\mathbf{u}_{j,3}\|_V$	unstable	unstable	unstable	1.22473	1.22473
	$\|\mathbf{u}_{j+1,0} - \mathbf{u}_{j,0}\|_V$		3.84e-07	2.40e-08	1.50e-09	9.38e-11
	$\|\mathbf{u}_{j+1,1} - \mathbf{u}_{j,1}\|_V$			6.99e-08	4.37e-09	2.73e-10
	$\|\mathbf{u}_{j+1,2} - \mathbf{u}_{j,2}\|_V$				1.24e-08	7.77e-10
	$\|\mathbf{u}_{j+1,3} - \mathbf{u}_{j,3}\|_V$					2.92e-09
	$f_{j,0}$			16.0022	16.0011	16.0005
	$f_{j,1}$				16.0006	16.0003
	$f_{j,2}$					16.0003
	$\|\mathbf{u}_{j,1} - \mathbf{u}_{j,0}\|_V$		1.80e-01	1.80e-01	1.80e-01	1.80e-01
	$\|\mathbf{u}_{j,2} - \mathbf{u}_{j,1}\|_V$			2.46e-02	2.46e-02	2.46e-02
	$\|\mathbf{u}_{j,3} - \mathbf{u}_{j,2}\|_V$				4.66e-03	4.66e-03

Table 1 Estimated convergence in time (evaluated at the final time T) and space for explicit Runge-Kutta methods with two or four stages for the example of Section 6.1

.

For this example the exact solution is not known. To study the convergence of the time integrator, we consider the approximated error $\|\mathbf{u}_{j+1,l} - \mathbf{u}_{j,l}\|_V$. The spatial error on level l is estimated by $\|\mathbf{u}_{j,l+1} - \mathbf{u}_{j,l}\|_V$.

Explicit Runge-Kutta methods We test the second and the fourth order method ($m = 2$ and $m = 4$) with $K_j = 3\,200 \cdot 2^j$ time steps, $j = 0, \ldots, 4$. The results are presented in Tab. 1. Due to the small elements in the tapered region of the spatial domain, the CFL condition requires small time steps. The order of convergence of the time integrator on the mesh of level l can be estimated from the factor

$$f_{j,l} = \frac{\|\mathbf{u}_{j-1,l} - \mathbf{u}_{j-2,l}\|_V}{\|\mathbf{u}_{j,l} - \mathbf{u}_{j-1,l}\|_V} \approx 2^m.$$

As can be seen from Tab. 1, the time integration shows the expected order two and four. However, even for the second order method, the error in space dominates the time discretization error in this example. Hence it is sufficient to use time steps which just match the CFL condition. Neither a further reduction of the time step nor using a higher order method improve the overall accuracy. The regularity in space is limited by the regularity of the initial function $\mathbf{u}_0 \in \mathrm{H}^2(\Omega)^3 \setminus \mathrm{H}^3(\Omega)^3$, so that we observe a convergence factor between 4 and 8 for quadratic elements in space.

Next, we investigate the overall convergence in space and time. Since Tab. 1 confirms that the numerically observed order of the time discretization coincides with the theoretically expected order, we can construct a better approximation of the semi-discrete solution $\mathbf{u}_l\colon [0,T] \longrightarrow V_l$ by extrapolation as

$$\mathbf{u}_l(T) \approx \mathbf{u}_l^{\text{ex}} = \frac{f_{J,l}}{f_{J,l}-1}\mathbf{u}_{J,l} - \frac{1}{f_{J,l}-1}\mathbf{u}_{J-1,l}\,.$$

In a second step, extrapolation in space yields the approximation

$$\mathbf{u}(T) \approx \mathbf{u}^{\text{ex}} = \frac{f}{f-1}\mathbf{u}_L^{\text{ex}} - \frac{1}{f-1}\mathbf{u}_{L-1}^{\text{ex}} \in V_L, \qquad f = \frac{\|\mathbf{u}_{L-1}^{\text{ex}} - \mathbf{u}_{L-2}^{\text{ex}}\|_V}{\|\mathbf{u}_L^{\text{ex}} - \mathbf{u}_{L-1}^{\text{ex}}\|_V}.$$

The results shown in Tab. 2 confirm that the total error for the explicit methods is dominated by the error in space.

	$\|\mathbf{u}_{0,l} - \mathbf{u}^{\text{ex}}\|_V$	$\|\mathbf{u}_{1,l} - \mathbf{u}^{\text{ex}}\|_V$	$\|\mathbf{u}_{2,l} - \mathbf{u}^{\text{ex}}\|_V$	$\|\mathbf{u}_{3,l} - \mathbf{u}^{\text{ex}}\|_V$	$\|\mathbf{u}_{4,l} - \mathbf{u}^{\text{ex}}\|_V$	$\|\mathbf{u}_l^{\text{ex}} - \mathbf{u}^{\text{ex}}\|_V$
$m=2$	$K_0 = 3\,200$	$K_1 = 6\,400$	$K_2 = 12\,800$	$K_3 = 25\,600$	$K_4 = 51\,200$	
$l=0$	1.99e-1	1.97e-1	1.97e-1	1.96e-1	1.97e-1	1.97e-1
$l=1$		2.81e-2	2.76e-2	2.75e-2	2.75e-2	2.75e-2
$l=2$			5.86e-3	5.75e-3	5.73e-3	5.73e-3
$l=3$				1.08e-3	1.09e-3	1.08e-3
$m=4$	$K_0 = 3\,200$	$K_1 = 6\,400$	$K_2 = 12\,800$	$K_3 = 25\,600$	$K_4 = 51\,200$	
$l=0$	1.97e-1	1.97e-1	1.97e-1	1.97e-1	1.97e-1	1.97e-1
$l=1$		2.75e-2	2.75e-2	2.75e-2	2.75e-2	2.75e-2
$l=2$			5.75e-3	5.75e-3	5.75e-3	5.75e-3
$l=3$				1.09e-3	1.09e-3	1.09e-3

Table 2 Error estimates by extrapolation in space and time for second and fourth order explicit Runge-Kutta methods.

Implicit Runge-Kutta methods We test the Gauß methods with $m = 1$ and $K_j = 800 \cdot 2^j$ and with $m = 3$ and $K_j = 32 \cdot 2^j$. Again, the convergence properties are investigated by extrapolation, see Tab. 3. Since Gauß methods are A-stable, they remain stable for any positive time step and thus the experiments use significantly fewer time steps than for the explicit Runge-Kutta methods: 12800 time steps for $m = 1$ and only 512 time steps for $m = 3$ are required on level $l = 3$ to obtain approximately the same accuracy estimate in time as in space.

	$\|\mathbf{u}_{0,l} - \mathbf{u}^{\text{ex}}\|_V$	$\|\mathbf{u}_{1,l} - \mathbf{u}^{\text{ex}}\|_V$	$\|\mathbf{u}_{2,l} - \mathbf{u}^{\text{ex}}\|_V$	$\|\mathbf{u}_{3,l} - \mathbf{u}^{\text{ex}}\|_V$	$\|\mathbf{u}_{4,l} - \mathbf{u}^{\text{ex}}\|_V$	$\|\mathbf{u}_l^{\text{ex}} - \mathbf{u}^{\text{ex}}\|_V$
$m=1$	$K_0 = 800$	$K_1 = 1600$	$K_2 = 3200$	$K_3 = 6400$	$K_4 = 12800$	
$l=0$	1.89e-1	1.92e-1	1.96e-1	1.97e-1	1.97e-1	1.97e-1
$l=1$	1.01e-1	3.44e-2	2.72e-2	2.75e-2	2.80e-2	2.85e-2
$l=2$	1.09e-1	2.99e-2	9.05e-3	5.85e-3	5.70e-3	5.74e-3
$l=3$	1.09e-1	3.15e-2	8.79e-3	2.48e-3	1.19e-3	1.05e-3
$m=3$	$K_0 = 32$	$K_1 = 64$	$K_2 = 128$	$K_3 = 256$	$K_4 = 512$	
$l=0$	3.88e-1	1.92e-1	1.96e-1	1.97e-1	1.97e-1	1.97e-1
$l=1$	4.89e-1	4.95e-2	2.72e-2	2.75e-2	2.76e-2	2.76e-2
$l=2$		5.78e-2	9.45e-3	5.73e-3	5.79e-3	5.79e-3
$l=3$		5.89e-2	1.11e-3	2.00e-3	1.15e-3	1.10e-3

Table 3 Convergence estimates by extrapolation in space and time for Gauß methods with $m = 1$ and $m = 3$ stages of order $2m$.

We clearly observe that implicit methods require far less time steps then explicit methods in order to reach the full accuracy in time and space. On the other hand, m large linear systems have to be solved in each time step of an m-stage method. In Tab. 4 we list the overall number of required preconditioning steps. Here, the 3-stage method is more efficient (with resepct to the number of preconditioning steps) than the second order implicit midpoint rule.

$m=1$	$K_0=800$	$K_1=1600$	$K_2=3200$	$K_3=6400$	$K_4=12800$
$l=0$	3178	5325	9600	19200	38400
$l=1$	3708	6384	10885	19200	38400
$l=2$	5408	7457	12763	22099	38400
$l=3$	6731	9147	14181	25517	39020
$m=3$	$K_0=32$	$K_1=64$	$K_2=128$	$K_3=256$	$K_4=512$
$l=0$	2273	3218	4821	7746	12786
$l=1$	3501	5469	6931	9809	15478
$l=2$	4298	7552	10598	13163	19534
$l=3$	4480	8653	14749	19339	24255

Table 4 Total number of preconditioning steps for solving mK_j linear systems $(\gamma\mathbb{M}+\tau\mathbb{A})v=b$ with a Gauß method with $m=1$ and $m=3$ stages.

Polynomial Krylov methods Alg. 1 is tested with MaxIter $=150$ and Tol $=10^{-5}$. Here, the restriction of the time step size τ comes from the fact that the limit of MaxIter $=150$ is exceeded if τ is too large. Note that in the case that the method is converging within MaxIter time steps, a further reduction of τ leads to a corresponding reduction of Krylov steps. Hence the overall efficiency is similar for a broad range of time step sizes giving the same accuracy for the final solution in space, cf. Tab. 5 and 6.

	$K_0=64$	$K_1=128$	$K_2=256$	$K_3=512$	$K_4=1024$
$l=0$	2739	2898	3268	3696	5128
$l=1$	5415	5568	5838	6254	7489
$l=2$	no conv.	11236	11484	11946	12595
$l=3$	no conv.	no conv.	23493	23989	24671

Table 5 Total number of multiplications with $\mathbb{M}^{-1}\mathbb{A}$ for the polynomial Krylov method.

	$\|\mathbf{u}_{0,l}-\mathbf{u}^{\text{ex}}\|_V$	$\|\mathbf{u}_{1,l}-\mathbf{u}^{\text{ex}}\|_V$	$\|\mathbf{u}_{2,l}-\mathbf{u}^{\text{ex}}\|_V$	$\|\mathbf{u}_{3,l}-\mathbf{u}^{\text{ex}}\|_V$	$\|\mathbf{u}_{4,l}-\mathbf{u}^{\text{ex}}\|_V$	$\|\mathbf{u}^{\text{ex}}_l-\mathbf{u}^{\text{ex}}\|_V$
$l=0$	1.97e-1	1.97e-1	1.97e-1	1.97e-1	1.97e-1	1.98e-1
$l=1$	2.80e-2	2.81e-2	2.83e-2	2.83e-2	2.82e-2	2.84e-2
$l=2$		6.63e-3	6.96e-3	6.69e-3	6.73e-3	6.81e-3
$l=3$			2.85e-3	1.89e-3	1.61e-3	1.47e-3

Table 6 Convergence estimates by extrapolation in space and time for the polynomial Krylov method.

Rational Krylov methods Alg. 2 is tested with several parameters, and for all tests in Tab. 6.1 we set MaxIter $=150$, Tol $=10^{-5}$, and $\gamma=20$. Similar results have been observerd with $\gamma\in(5,20)$. A conservative choice would be $\gamma=2$ which corresponds to using the same denominator polynomial as for the implicit midpoint rule. Experimentally we found that larger values of γ increased the efficiency of the algorithm.

For the rational Krylov method we use a smaller tolerance Tol than in the polynomial case, since otherwise the approximation (24) is not accurate enough. On the finest level the full accuracy in space is already obtained with 64 time steps and less than 15 000 preconditioning steps.

	$K_0=16$	$K_1=32$	$K_2=64$	$K_3=128$	$K_4=256$
$l=0$	390 (2540)	514 (2823)	758 (3475)	1161 (4513)	1728 (6350)
$l=1$	593 (4502)	667 (4433)	964 (5140)	1483 (6425)	2244 (8214)
$l=2$	1064 (9339)	963 (7757)	1178 (7855)	1860 (9376)	2946 (11844)
$l=3$	1974 (19742)	1581 (16301)	1630 (14399)	2215 (14238)	3319 (16279)

Table 7 Total number of approximate solutions of $(\gamma\mathbb{M}+\tau\mathbb{A})v=b$ (and total number of preconditioning steps) for the rational Krylov method with $\gamma=20$, $\tau=T/K_j$ and $T=8$.

	$\|\mathbf{u}_{0,l} - \mathbf{u}^{\text{ex}}\|_V$	$\|\mathbf{u}_{1,l} - \mathbf{u}^{\text{ex}}\|_V$	$\|\mathbf{u}_{2,l} - \mathbf{u}^{\text{ex}}\|_V$	$\|\mathbf{u}_{3,l} - \mathbf{u}^{\text{ex}}\|_V$	$\|\mathbf{u}_{4,l} - \mathbf{u}^{\text{ex}}\|_V$	$\|\mathbf{u}_l^{\text{ex}} - \mathbf{u}^{\text{ex}}\|_V$
$l = 0$	6.56e3	1.97e-1	1.97e-1	1.97e-1	1.97e-1	1.97e-1
$l = 1$	7.55e3	2.75e-2	2.76e-2	2.76e-2	2.76e-2	2.76e-2
$l = 2$	5.76e3	5.76e-3	5.76e-3	5.76e-3	5.76e-3	5.76e-3
$l = 3$	1.54e3	1.36e-3	1.09e-3	1.09e-3	1.09e-3	1.09e-3

Table 8 Convergence estimates by extrapolation in space and time for the rational Krylov method.

Comparison The computational results (evaluated by counting the number of matrix operations) show clearly that for this example the polynomial Krylov method is far more efficient than fixed order explicit Runge-Kutta methods. This is confirmed by the parallel execution time* in Tab. 9. In all explicit methods, the required number of steps is proportional to 2^l, since the CFL condition requires $O(\tau) = O(h)$. For the implicit methods, the required number of time steps is independent of the spatial discretization, see [22] for a rigorous error analysis for Maxwell equations. Obviously, implicit Runge-Kutta methods and rational Krylov methods are only more efficient than explicit methods, if a suitable preconditioner is available. Nevertheless, even without using an optimized preconditioner, our results show that implicit methods outperform explicit even on the coarse grids. The advantage of implicit methods over explicit ones becomes significant on finer grids.

In general, we found that the Krylov methods are not very sensitive with respect to the choice of the time step size (the computational cost is almost constant for the polynomial Krylov methods for different time steps).

explicit Runge-Kutta method $m = 4$	$K_0 = 3\,200$	$K_1 = 6\,400$	$K_2 = 12\,800$	$K_3 = 25\,600$	$K_4 = 51\,200$
$l = 0$	0:12	0:25	0:49	1:39	3:20
$l = 1$		1:17	2:34	5:17	10:32
$l = 2$			9:31	19:31	39:03
$l = 3$				134:56	270:27
implicit Runge-Kutta method $m = 1$	$K_0 = 800$	$K_1 = 1600$	$K_2 = 3200$	$K_3 = 6400$	$K_4 = 12800$
$l = 0$	0:12	0:21	0:40	1:20	2:41
$l = 1$	0:28	0:49	1:25	2:41	5:23
$l = 2$	1:43	2:40	4:34	8:20	15:46
$l = 3$	6:58	10:20	17:13	30:03	53:15
implicit Runge-Kutta method $m = 3$	$K_0 = 32$	$K_1 = 64$	$K_2 = 128$	$K_3 = 256$	$K_4 = 512$
$l = 0$	0:14	0:20	0:30	0:50	1:24
$l = 1$	0:47	1:13	1:38	2:24	3:55
$l = 2$	2:56	5:11	7:26	9:51	15:02
$l = 3$	10:15	19:35	32:53	43:07	57:07
polynomial Krylov method	$K_0 = 64$	$K_1 = 128$	$K_2 = 256$	$K_3 = 512$	$K_4 = 1024$
$l = 0$	0:06	0:06	0:06	0:09	0:14
$l = 1$	0:46	0:29	0:27	0:34	0:47
$l = 2$		2:51	2:09	2:17	2:55
$l = 3$			24:31	20:34	21:02
rational Krylov method	$K_0 = 16$	$K_1 = 32$	$K_2 = 64$	$K_3 = 128$	$K_4 = 256$
$l = 0$	0:13	0:18	0:29	0:49	1:28
$l = 1$	0:36	0:40	0:54	1:21	2:11
$l = 2$	3:09	2:43	3:00	3:59	5:46
$l = 3$	21:48	17:46	16:25	17:46	22:56

Table 9 Comparison of the parallel execution time in minutes (128 processes) for the full simulation of the 2D Maxwell example.

6.2 Maxwell equation in 3D

In the second example, we study a resonator configuration in $\Omega \subset (0, 1088) \times (-133, -133) \times (-133, -133)$ using an unstructured tetrahedral mesh. Some snapshots of the $\mathbf{H}_y$ component of the magnetic field are shown in Fig. 2. The

* Since M++ is general purpose parallel finite element code, it is not optimized for discontinuous Galerkin methods with explicit time stepping; a more efficient implementation which is specially designed for this problem class is introduced, e.g., in [25].

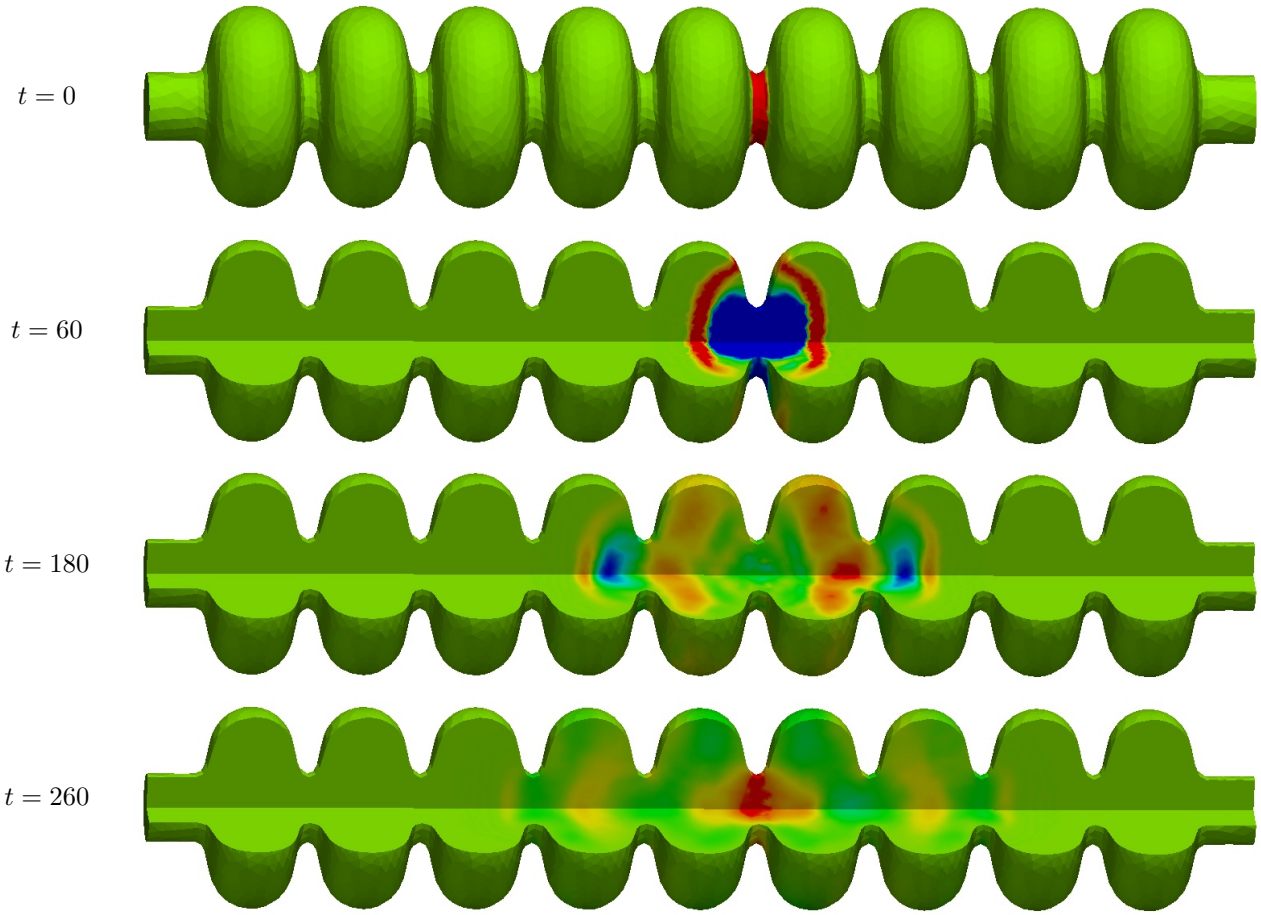

Fig. 2 Initial distribution of $\mathbf{H}_y$ and time evolution at selected time steps for one resonance period on the planes $y = 0$ and $z = 0$.

DG discretization on 1 045 072 tetrahedra with quadratic elements leads to a system of 62 704 320 ordinary differential equations. For the simulation we used a polynomial Krylov subspace method with 30 time steps, which required a total number of 3449 Krylov steps. The computation on 96 processor kernels took about 7:10 hours.

6.3 Elastic wave equation in 2D

In this example we consider a configuration motivated by a new technique in seismic tunnel exploration [23]: an artificially generated surface wave in the tunnel propagates into the solid, and measurements of the reflected shear wave turned out to be a successful forward looking approach. In Fig. 3 we show the approximate solutions of the 2d elastic wave equation with Lamé parameters $\mu = 1$ and $\lambda = 3$ on the domain $\Omega \subset (-2, 2) \times (-4.5, 3.25)$. For these parameters, the pressure wave is significantly faster than the shear wave. Note that the domain is quite large so that the (artificial) reflections from the other boundaries do not interact with the first reflected shear wave front.

For the simulation we use discontinuous Galerkin elements of degree $p = 1$ on a mesh with 528 384 triangles resulting in 7 925 760 degrees of freedom. The full simulation requires a total of 16 706 Krylov steps for the polynomial Krylov method. A detailed study of the convergence in time and space is given in [34].

In this application we are only interested in a high resolution near the tunnel. This can be achieved by adaptivity or non-reflection boundary techniques. The combination of these methods with the efficient time integrators discussed in this paper will be reported elsewhere.

6.4 Conclusion

In this paper we have shown our first numerical experiments illustrating the efficiency of different time integration schemes for solving wave equations discretized by discontinuous Galerkin methods. We have explained theoretically and verified

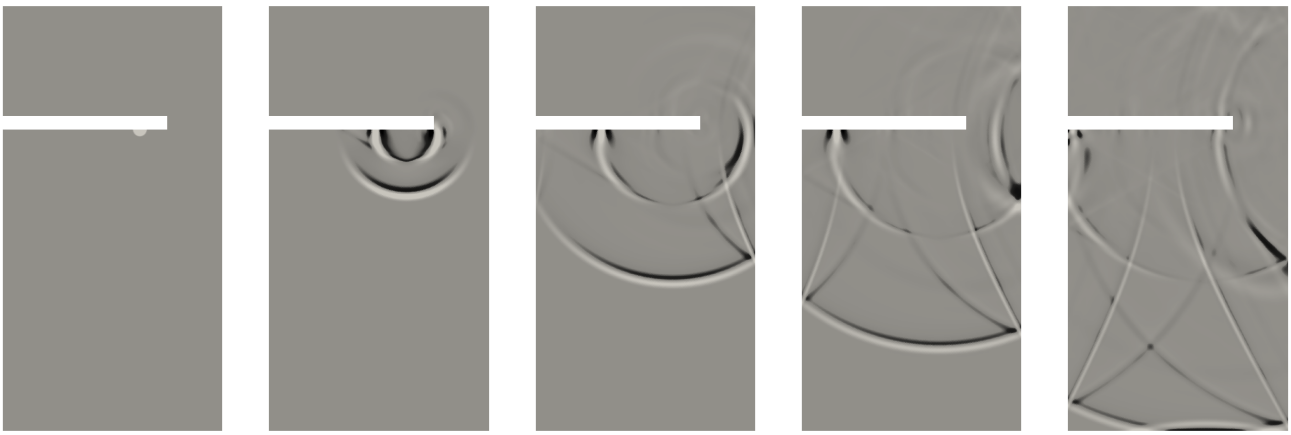

Fig. 3 Distribution of the velocity component $\mathbf{v}_y$ at sample time steps. The starting impulse at the tunnel surface ($t = 0$) induces two wave fronts, a shear wave and a pressure wave ($t = 0.6$). The shear ware reaches the right boundary ($t = 1.4$) and is reflected ($t = 2$). This can be measured at the tunnel boundary as surface wave ($t = 2.8$).

numerically that polynomial Krylov subspace methods clearly outperform standard explicit Runge-Kutta methods. Moreover, even though our implementation of solving the linear systems arising in implicit Runge-Kutta or rational Krylov methods was not optimized for the particular application, the results show that implicit methods can outperform explicit schemes in particular on fine grids. This shows the great potential of implicit schemes for linear wave equations. However, much more research is necessary to provide optimal (multigrid) preconditioners for the linear systems and to determine the parameters τ and γ to minimize the overall computational time. Moreover, a reliable error control has to be developed to balance the error in space and time and to determine suitable bounds for the truncation error of iterative solvers. This is a topic of our future research.

Acknowledgments

We thank the referees for the helpful suggestions which improved this work. We gratefully acknowledge the support of the German Research Foundation (DFG) by GRK 1294 and FOR 1650.

References

[1] A. H. Al-Mohy and N. J. Higham, Computing the action of the Matrix exponential, with an application to exponential integrators, SIAM J. Sci. Comp. **33**(2), 488–511 (2011).
[2] M. A. Botchev, V. Grimm, and M. Hochbruck, Residual, Restarting, and Richardson Iteration for the Matrix Exponential, SIAM J. Sci. Comput. **35**(3), A1376–A1397 (2013).
[3] M. Botchev, D. Harutyunyan, and J. Van der Vegt, The Gautschi time stepping scheme for edge finite element discretizations of the Maxwell equations, Journal of Computational Physics **216**(2), 654–686 (2006).
[4] E. Burman, A. Ern, and M. A. Fernández, Explicit Runge-Kutta schemes and finite elements with symmetric stabilization for first-order linear PDE systems, SIAM J. Numer. Anal. **48**(6), 2019–2042 (2010).
[5] M. H. Chen, B. Cockburn, and F. Reitich, High-order RKDG methods for computational electromagnetics, Journal of Scientific Computing **22**(1-3), 205–226 (2005).
[6] D. A. Di Pietro and A. Ern, Mathematical aspects of discontinuous Galerkin methods, Mathématiques & Applications (Berlin) [Mathematics & Applications], Vol. 69 (Springer, Heidelberg, 2012).
[7] V. Druskin and R. Remis, A Krylov stability-corrected coordinate-stretching method to simulate wave propagation in unbounded domains, SIAM Journal on Scientific Computing **35**(2), B376–B400 (2013).
[8] M. Eiermann, O. Ernst, and S. Güttel, Deflated restarting for matrix functions, SIAM Journal on Matrix Analysis and Applications **32**(2), 621–641 (2011).
[9] K. J. Engel and R. Nagel, A short course on operator semigroups, Universitext (Springer, New York, 2006).
[10] L. Fezoui, S. Lanteri, S. Lohrengel, and S. Piperno, Convergence and stability of a discontinuous Galerkin time-domain method for the 3d heterogeneous Maxwell equations on unstructured meshes, M2AN Math. Model. Numer. Anal. **39**(6), 1149–1176 (2005).
[11] E. Gallopoulos and Y. Saad, Efficient solution of parabolic equations by Krylov approximation methods, SIAM J. Sci. Statist. Comput. **13**(5), 1236–1264 (1992).

[12] T. Göckler and V. Grimm, Convergence Analysis of an Extended Krylov Subspace Method for the Approximation of Operator Functions in Exponential Integrators, SIAM J. Numer. Anal. **51**(4), 2189–2213 (2013).
[13] S. Gottlieb, C. W. Shu, and E. Tadmor, Strong stability-preserving high-order time discretization methods, SIAM Review **43**(1), 89–112 (2001).
[14] V. Grimm, Resolvent Krylov subspace approximation to operator functions, BIT Numerical Mathematics **52**(3), 639–659 (2012).
[15] M. J. Grote and T. Mitkova, Explicit local time-stepping methods for Maxwells equations, Journal Comput. and Appl. Math. **234**(12), 3283–3302 (2010).
[16] S. Güttel, Rational Krylov approximation of matrix functions: Numerical methods and optimal pole selection, GAMM-Mitteilungen **36**(1), 8–31 (2013).
[17] E. Hairer and G. Wanner, Solving Ordinary Differential Equations II. Stiff and Differential-Algebraic Problems, 2nd edition, Springer Series in Computational Mathematics, Vol. 14 (Springer, Berlin, Heidelberg, 1996).
[18] J. S. Hesthaven and T. Warburton, Nodal discontinuous Galerkin methods, Texts in Applied Mathematics, Vol. 54 (Springer, New York, 2008), Algorithms, analysis, and applications.
[19] J. Hesthaven and T. Warburton, Nodal high-order methods on unstructured grids. I: Time-domain solution of Maxwell's equations., J. Comput. Phys. **181**(1), 186–221 (2002).
[20] N. J. Higham, Functions of matrices (Society for Industrial and Applied Mathematics (SIAM), Philadelphia, PA, 2008), Theory and computation.
[21] M. Hochbruck and C. Lubich, On Krylov subspace approximations to the matrix exponential operator, SIAM J. Numer. Anal. **34**(5), 1911–1925 (1997).
[22] M. Hochbruck and T. Pažur, Implicit Runge–Kutta methods and discontinuous Galerkin discretizations for linear Maxwell's equations, Tech. rep., Karlsruhe Institute of Technology, 2013.
[23] S. Jetschny, T. Bohlen, and D. De Nil, On the propagation characteristics of tunnel surface-waves for seismic prediction, Geophysical Prospecting **58**(2), 245–256 (2010).
[24] M. Käser and M. Dumbser, An arbitrary high-order discontinuous Galerkin method for elastic waves on unstructured meshes – I. The two-dimensional isotropic case with external source terms, Geophys. J. Int. **166**, 855–877 (2006).
[25] A. Klöckner, T. Warburton, J. Bridge, and J. S. Hesthaven, Nodal discontinuous Galerkin methods on graphics processors, Journal of Computational Physics **228**(21), 7863–7882 (2009).
[26] L. Krivodonova, An efficient local time-stepping scheme for solution of nonlinear conservation laws, Journal Comput. Phys. **229**(22), 8537–8551 (2010).
[27] R. J. Leveque, Finite volume methods for hyperbolic problems. (Cambridge: Cambridge University Press, 2002).
[28] H. Luo, J. D. Baum, and R. Löhner, A p-multigrid discontinuous Galerkin method for the Euler equations on unstructured grids, Journal of Computational Physics **211**(2), 767–783 (2006).
[29] D. Maurer and C. Wieners, A parallel block LU decomposition method for distributed finite element matrices, Parallel Computing **37**, 742–758 (2011).
[30] R. F. Remis and P. M. Van den Berg, A modified Lanczos algorithm for the computation of transient electromagnetic wavefields, Microwave Theory and Techniques, IEEE Transactions on **45**(12), 2139–2149 (1997).
[31] M. Renardy and R. C. Rogers, An introduction to partial differential equations. 2nd ed. (New York, NY: Springer, 2004).
[32] Y. Saad, Analysis of some Krylov subspace approximations to the matrix exponential operator, SIAM J. Numer. Anal. **29**(1), 209–228 (1992).
[33] D. Sármány, M. Botchev, and J. J. van der Vegt, Dispersion and dissipation error in high-order Runge-Kutta discontinuous Galerkin discretisations of the Maxwell equations, Journal of Scientific Computing **33**(1), 47–74 (2007).
[34] R. Shirazi-Najad, Ein discontinuous Galerkin Verfahren für Wellenausbreitung in elastischen Medien (Karlsruhe Institue of Technology, 2013), diploma thesis.
[35] R. B. Sidje, EXPOKIT: a software package for computing matrix exponentials, ACM Trans. Math. Softw. **24**(1), 130–156 (1998).
[36] A. Taube, M. Dumbser, C. D. Munz, and R. Schneider, A high-order discontinuous Galerkin method with time-accurate local time stepping for the Maxwell equations, International Journal of Numerical Modelling: Electronic Networks, Devices and Fields **22**(1), 77–103 (2009).
[37] J. van den Eshof and M. Hochbruck, Preconditioning Lanczos approximations to the matrix exponential, SIAM J. Sci. Comput. **27**(4), 1438–1457 (2006).
[38] J. P. Vila and P. Villedieu, Convergence of an explicit finite volume scheme for first order symmetric systems., Numer. Math. **94**(3), 573–602 (2003).
[39] C. Wieners, A geometric data structure for parallel finite elements and the application to multigrid methods with block smoothing, Computing and Visualization in Science **13**, 161–175 (2010).
[40] C. Wieners, Distributed point objects. A new concept for parallel finite elements, in: Domain decomposition methods in science and engineering, edited by R. Kornhuber, R. Hoppe, J. Périaux, O. Pironneau, O. Widlund, and J. Xu, Lect. Notes Comput. Sci. Eng. Vol. 40 (Springer, Berlin, 2005), pp. 175–182.
[41] M. Zaslavsky and V. Druskin, Solution of time-convolutionary Maxwell's equations using parameter-dependent Krylov subspace reduction, Journal of Computational Physics **229**(12), 4831–4839 (2010).